9-1-2015

Examining the effects of a sub-chronic exposure to phencyclidine: An analysis of functional network connectivity, behavior, and mRNA expression

Christy M. Magcalas

Christy M. Magcalas
Candidate

Psychology
Department

This thesis is approved, and it is acceptable in quality and form for publication:

Approved by the Thesis Committee:

Dr. Derek A. Hamilton , Chairperson

Dr. Nora Perrone-Bizzozero

Dr. Vince D. Calhoun

Dr. Juan Bustillo

Examining the effects of a sub-chronic exposure to phencyclidine: An analysis of functional network connectivity, behavior, and mRNA expression

by

Christy M. Magcalas

B.A., Psychology, University of Nevada, Las Vegas, 2012

THESIS

Submitted in Partial Fulfillment of the

Requirements for the Degree of

Master of Science
Psychology

The University of New Mexico

Albuquerque, New Mexico

July, 2015

Dedication

For my parents, Deo and Nina Magcalas, and my siblings, Caroline, Cheryl, and Philip.

Acknowledgments

I would like to begin by acknowledging my mentor and thesis committee chair, Dr. Derek Hamilton. He has supplied me with endless amounts of knowledge, patience, and support and continues to do so throughout my graduate career. I appreciate all of the opportunities that Dr. Hamilton has given me, such as accepting me into his laboratory as a graduate student, helping me get involved with a host of research projects, and giving me an environment to thrive in. I owe a majority of my success to his excellent mentoring skills and to his confidence in me. I could not have asked for a better mentor for my graduate career.

Next, I would like acknowledge my thesis committee, Dr. Nora Perrone-Bizzozero, Dr. Vince D. Calhoun, and Dr. Juan Bustillo. I am grateful for their knowledge and feedback throughout my thesis experience. I would like to specifically thank Dr. Perrone-Bizzozero for the unlimited amount help and kindness that she shared with me throughout this project. Also, I would like to recognize the members of the Perrone-Bizzozero Laboratory, especially Rob Oliver who never failed to assist with any question or problem that arose while I was collecting data.

In addition, I would like to acknowledge my fellow Hamilton Laboratory members: Dr. Clark Bird, Dan Barto, and Carlos Rodriguez. They have consistently been excellent sources of knowledge, support, and feedback throughout my graduate career. Also, I would like to recognize my undergraduate laboratory's members: Dr. Jefferson Kinney, Dr. Chelcie Heaney, Monica Bolton, and Andrew Murtishaw. Without them I would have never been able to establish a foundation in research that ultimately lead me to graduate school.

Finally, I would like to recognize my family. My parents, Nina and Deo Magcalas, have always been supportive throughout my unorthodox path to where I am today. They have always dedicated their lives to enhancing the lives of all of those around them. My siblings, Caroline, Cheryl, and Philip, and my sister-in-law, Lucy, have been inspirations to me throughout my life. I do not know where I would be without my family's love and, for that, I would like to thank them.

Examining the effects of a sub-chronic exposure to phencyclidine: An analysis of functional network connectivity, behavior, and mRNA expression

by

Christy M. Magcalas

B.A., Psychology, University of Nevada, Las Vegas, 2012

M.S., Psychology, University of New Mexico, 2015

Abstract

Glutamate is the primary excitatory neurotransmitter in the central nervous system and plays a vital role in the pathology of various disease states. Thus, the manipulation and examination of glutamate has been and continues to be pivotal in experimental research. For example, a chronic administration of phencyclidine (PCP), a non-competitive glutamatergic N-methyl-D-Aspartate (NMDA) receptor antagonist, generates behavioral and neurobiological changes that mimic symptoms and micro-level changes found in psychiatric disease states, such as schizophrenia [30]. Prior research has established that PCP induces cognitive deficits, impedes spatial learning and memory performance, and alters mRNA expression of γ-aminobutyric acid (GABA)ergic markers parvalbumin, GAD_{67}, calbindin, and tyrosine kinase ErbB4 in addition to glutamate NMDA receptor subunits GluN2A and GluN2B in ways that are comparable to findings in the schizophrenia population [10, 11, 18, 48]. Recently, a growing interest in observing functional network connectivity (FNC) has lead to

innovative ways of examining both normal systems and disease states. FNC imaging has successfully identified similar networks in both humans and rats [29] which has motivated translational research. Yet, little research has examined the effects of PCP on FNC in an animal system.

In the current study, we characterized how a sub-chronic administration of PCP can manipulate FNC and how those changes relate to observed behavioral and mRNA expression outcomes. Adult male hooded Long Evan rats (N=40) were pre-trained in the hidden platform Morris water task (MWT) prior to beginning their chronic treatment. Rats received 14 intraperitoneal (i.p.) injections of either PCP (2.58 mg/kg/injection) or 0.9% saline solution (1 mL/kg) over a period of 26 days. Seventy-two hours after the final injection all animals were anesthetized with isoflurane and imaged in a 4.7 T Bruker Biospin MRI Scanner. Fast spin-echo anatomical scans, resting state functional magnetic resonance imaging (fMRI) scans with echo-planar imaging (EPI) acquisition sequences, and arterial spin labeling (ASL) scans were acquired during the one-hour imaging session. On day 36, 10 days following the final injection, a subset of animals (PCP treated n=10, saline treated n=10) were rescanned to examine the effects of a one week washout period. Following the final scan all animals were retested in the MWT. The animals were initially tested in 8 retraining trials. After a break of least an hour in their home cage, the animals were given a short retraining session consisting of 4 trials followed by 8 trials of reversal where the hidden platform was shifted 180^o from the trained location in order to examine behavioral flexibility. Upon completion of behavioral testing, the animals were sacrificed and tissue was collected and stored at -80^oC for GABA and NMDA receptor mRNA expression analysis.

Group differences in the individual components were assessed through comparisons of FNC (inter-component correlations) and spectral power comparisons. Group independent component analyses (ICA) were conducted through the implementation

of the Group ICA of fMRI Toolbox (GIFT). Additionally, select brain regions of interest, including the medial frontal cortex and ventral frontal cortex, were assessed for mRNA expression. Real-time polymerase chain reaction (RT-PCR) was used to assess mRNA expression of the GABAergic markers parvalbumin, calbindin, ErbB4, and GAD_{67}, as well as NMDA receptor subunits GluN2A and GluN2B. The expression of these receptors within the frontal cortex were compared to expression levels within the parietal cortex, which was used as a control region. These analyses were used to observe the neurobiological effects of a sub-chronic exposure to PCP. MWT data was analyzed to determine the effects of the treatments and to characterize learning and memory performance changes following a low dose sub-chronic administration of PCP. Finally, these behavioral data also allowed for the examination of behavioral differences between groups based on temporal proximity to cessation of PCP treatment. The PCP exposed animals displayed persistent connectivity changes and alterations in mRNA expression of parvalbumin, calbindin, and GAD_{67}.

Contents

List of Figures **x**

1 Specific Aims **1**

1.1 Aims 3

2 Introduction **4**

2.1 Functional Network Connectivity 5

2.2 N-methyl-D-aspartate (NMDA) Receptors 6

2.3 Behavioral Changes 8

2.4 Innovation 9

3 Materials and Methods **11**

3.1 Subjects 11

3.2 Drugs 12

3.3 Behavioral Testing 13

3.3.1 Hidden Platform Morris Water Task (MWT) 13

3.4 fMRI Scanning 16

3.5 Quantitative Real-Time PCR (qRT-PCR) 17

3.6 Analysis 18

4 Results **19**

4.1 Functional Network Connectivity (FNC) 19

4.1.1 Orientation To The Presentation Of The FNC Results 19

4.1.2 Components 20

4.1.3 Overall Functional Network Connectivity 21

4.1.4 FNC on Day 29 - Saline Exposed Animals 23

4.1.5 FNC on Day 29 - PCP Exposed Animals 24

4.1.6 FNC - Statistical Analysis of Treatment Effects on Day 29 . . 25

4.1.7 FNC on Day 36 - Saline Exposed Animals 27

4.1.8 FNC on Day 36 - PCP Exposed Animals 28

4.1.9 FNC - Statistical Analysis of Treatment Effects on Day 36 . . 29

4.1.10 FNC - Statistical Analysis of the Cessation Period on Saline Exposed Animals 30

4.1.11 FNC - Statistical Analysis of the Cessation Period on PCP Exposed Animals 32

4.2 Spectral Power Analyses 33

4.2.1 Orientation To The Presentation Of The Spectral Results . . . 33

4.2.2 Spectral Power - ANOVA Interactions 34

4.2.3 Spectral Power - ANOVA Treatment Main Effect 34

4.2.4 Spectral Power - ANOVA Time Point Main Effect 35

4.2.5 Spectral Power - Statistical Analyses of Treatment Effects . . 35

4.2.6 Spectral Power - Statistical Analysis of Cessation Period Effects 37

4.2.7 Spectral Power - Statistical Analyses of Treatment Effects on Day 29 37

4.2.8 Spectral Power - Statistical Analysis of Treatment Effects on Day 36 39

4.3 Morris Water Task 40

4.3.1 Pre-injection Training 41

4.3.2 Post-Injection Testing 41

4.3.3 MWT Retraining Final Scan on Day 29 43

4.3.4 MWT Retraining Final Scan on Day 36 43

4.3.5 MWT Reversal Final Scan on Day 29 44

4.3.6 MWT Reversal - Final Scan on Day 36 46

4.4 Quantitative Real-Time PCR Results 46

5 Discussion **50**

References **55**

List of Figures

3.1 Timeline of sub-chronic sub-intermittent treatment of PCP or saline, fMRI scanning, behavioral testing, and tissue collection. 12

4.1 Twenty-one non-artifactual components identified and used throughout functional network connectivity and spectral time course analyses. Component t-map images are composed of sagittal, coronal, and transverse views with a threshold of 3.7. Components are organized anterior to posterior within brain regions and based off of the peak t-value indicated by the yellow coloring. 21

4.2 Overall correlations matrix demonstrates which components are significantly different than zero when components are collapsed across both treatment conditions. 22

4.3 Day 29 FNC for saline exposed animals - correlations matrix demonstrates which components are significantly different than zero. White dots indicate significance at $p<0.00025$. Black dots indicate significance at $p<0.005$. 23

4.4 Day 29 FNC for PCP exposed animals - correlations matrix demonstrates which components are significantly different than zero.White dots indicate significance at p<0.00025. Black dots indicate significance at p<0.005. 25

4.5 T-test conducted to determine treatment effects occurring on day 29. The saline data were subtracted from the PCP data (PCP-Sal) in order to determine the differences between the treatment groups. Black dots indicate significance at p<0.005. 26

4.6 Day 36 FNC for saline exposed animals - correlations matrix demonstrates which components are significantly different than zero. White dots indicate significance at p<0.00025. Black dots indicate significance at p<0.005. 27

4.7 Day 36 FNC for PCP exposed animals - correlations matrix demonstrates which components are significantly different than zero. White dots indicate significance at p<0.00025. Black dots indicate significance at p<0.005. 28

4.8 T-test conducted to determine treatment effects occurring on day 36. The saline data were subtracted from the PCP data (PCP-Sal) in order to determine the differences between the treatment groups. Black dots indicate significance at p<0.005. 30

4.9 T-tests conducted to determine the effects of the 1 week washout period in the saline exposed rats. The data from day 36 were subtracted from the data from day 29 (Day 29-Day 36) in order to determine the differences between the two scan time points. Black dots indicate significance at p<0.005. 31

4.10 T-tests conducted to determine the effects of the 1 week washout period in the PCP exposed rats. The data from day 36 were subtracted from the data from day 29 (Day 29-Day 36) in order to determine the differences between the two scan time points. Black dots indicate significance at p<0.005. 32

4.11 ANOVA omnibus p-value maps conducted on spectral power. The separate figures indicate significant (A) interactions, (B) the main effects of treatment, and (C) the main effects of the time point. Red dots indicate significance at p<0.05 and blue dots indicate significance at p<0.05/6. 36

4.12 T-tests conducted to determine the effects of the treatment (A. PCP-Sal) and the 1 week washout period (B. Day 29-Day36). Black dots indicate significance at p<0.05 and white dots indicate significance at p<0.05/6. 38

4.13 T-tests conducted to determine treatment effects on day 29 (A) and day 36 (B). Black dots indicate significance at p<0.05 and white dots indicate significance at p<0.05/6. 40

4.14 Pre-injection MWT training collapsed across scan time groups within each treatment group. Saline exposed animals are indicated by the open diamonds and PCP exposed animals are indicated by the closed red squares. The dependent measures are the length of the swim path (cm, A) and latency (sec, B) to reach the hidden platform location. . 42

4.15 Post-injection MWT retraining for both treatment groups (A, B) without and (C, D) with the 1-week cessation period. Saline exposed animals are indicated by the open black and gray diamonds and PCP exposed animals are indicated by the closed red and pink squares. The dependent measures are the length of the swim path (cm, A and C) and latency (sec, B and D) to reach the hidden platform location. 45

4.16 Post-injection MWT reversal for both treatment groups (A, B) without and (C, D) with the 1-week cessation period. Saline exposed animals are indicated by the open black and gray diamonds and PCP exposed animals are indicated by the closed red and pink squares. The dependent measures are the length of the swim path (cm, A and C) and latency (sec, B and D) to reach the hidden platform location. 47

4.17 Summary of analyses investigating treatment main effects, time main effects, and treatment by scan time interactions in mRNA expression levels of calbindin, GAD67, parvalbumin, ErbB4, GluN2A, and GluN2B in the medial frontal cortex, ventral frontal cortex, and parietal cortex. 48

4.18 Relative mRNA expression levels of (A) parvalbumin and (B) GAD_{67} in the parietal cortex and (C) calbindin in the medial frontal cortex. 49

Chapter 1

Specific Aims

Changes in glutamatergic function and the transmission of glutamate have been associated with the pathophysiology of various diseases, such as anxiety disorders, major depression, bipolar disorder, Alzheimer's disease, and schizophrenia [24,43,46]. Specifically, one of the predominant theories of schizophrenia is based on findings that show how blocking N-methyl-D-aspartate (NMDA) type glutamate receptors produces schizophreia-like symptoms and deficits in both healthy humans and non-human mammals [31,37]. This NMDA hypothesis has been the foundation for many studies that use NMDA antagonists, such as ketamine, MK-801, and phencyclidine (PCP), to study changes in glutamate, γ-aminobutyric acid (GABA), and NMDA receptors as well as behavioral changes in possible animal models of schizophrenia. Manipulations of NMDA receptor function through injections of antagonists [40], partial antagonists [12], and mutating gene expressions [15] have altered learning and memory performance and cognitive abilities in various behavioral tasks, including the Morris Water Task (MWT), novel object recognition, and pre-pulse inhibition [44]. Additionally, prior research has found that repeated exposure to PCP alters the neurotransmission of glutamate and leads to the deficits of many GABAergic markers, such as parvalbumin, calbindin, ErbB4, and GAD_{67} and alterations to

glutamate NMDA containing 2A and 2B subunits receptors (GluN2A and GluN2B) [4, 10, 18, 44].

In recent years, research investigating functional network connectivity (FNC) and low frequency fluctuations in the blood-oxygen-level- dependent (BOLD) signal measured via functional magnetic resonance imaging (fMRI) have increased in order to characterize the components and networks in healthy and abnormal systems. Patients with schizophrenia display connectivity differences within regions of the brain that have been commonly associated with cognitive deficits found in the disease state, such as the dorsolateral prefrontal cortex and the temporal lobes [21]. Additionally, similar components and networks have been identified in human and animal fMRI analysis, which gives support for further translational work [14, 29]. Yet, the merger of a sub-chronic PCP model of schizophrenia and measures of FNC research has yet to be made. This type of research would help establish conditions for which PCP and the resulting alterations in glutamatergic function is a valid model of schizophrenia.

Toward these goals, two working hypotheses were developed:

A) Chronic administration of PCP will induce similar FNC changes in rats as those found in the clinical schizophrenia population.

B) The sequelae of PCP exposure that mimic states observed in schizophrenia (a decrease in mRNA expression of GABAergic markers parvalbumin, calbindin, ErbB4, and GAD_{67} and NMDA receptor subunits GluN2A and GluN2B) and behavioral alterations will be consistent with findings observed in the clinical schizophrenia population and other models utilize NMDA antagonism.

1.1 Aims

We propose several experiments organized into two specific aims to address these hypotheses.

Specific Aim 1 Does chronic exposure to PCP induce persistent changes in FNC and spectral power in a rodent system?

Experiment Series 1.1 Establish measurements of resting state BOLD signals and conduct analysis of FNC and power spectra comparisons of components identified using group ICA. Examine if these functional changes are comparable to changes found in the schizophrenia population and other models involving NMDA antagonism.

Specific Aim 2 Are changes in mRNA expression for NMDA and GABAergic receptors and behavioral outcomes translational to the clinical schizophrenia population and other established animal models?

Experiment Series 2.1 Determine the effects of PCP on mRNA expression of parvalbumin, calbindin, ErbB4, GAD_{67}, GluN2A, and GluN2B and determine if these findings are translational to the clinical population and comparable animal models.

Experiment Series 2.2 Determine the behavioral effects of sub-chronic PCP exposure through the MWT and determine if these effects mimic states observed in schizophrenia.

Chapter 2

Introduction

Experimental research with animals has played a vital role in characterizing pathologies and biomechanisms involved in disease states. Through the use of animals, researchers have been able to explore a breadth of changes within a system that can help further explain the possible etiologies of various diseases. Thus, establishing valid animal models plays a vital role in being able to characterize disease states compared to a typically developing and functioning system. For example, animal research has been pivotal in determining the neurobiomechanisms involved in schizophrenia. Schizophrenia is a serious psychopathology that affects 1% of the population. Schizophrenia is comprised of positive symptoms, negative symptoms, and cognitive deficits that usually arise during early adulthood, primarily around 18-25 years of age. More specifically, schizophrenia patients experience hallucinations and delusions (positive symptoms), sensorimotor gating deficits, auditory and visual context-dependent processing deficits, emotional processing deficits, and memory impairments (negative symptoms) in addition to information processing, working memory, and executive functioning disruptions and deficits (cognitive deficits) [30]. Schizophrenia compromises the health and well-being of those afflicted with this life-long disease and the etiology and pathophysiology are still unknown. Current

pharmacological treatments are centered around the blocking of dopamine D2 receptors through the administration of atypical antipsychotics. These treatments tend to address the psychotic symptoms, but neglect to alleviate one from the core cognitive dysfunctions [13]. Understanding the mechanisms involved in this disorder is vital in order to be able to work towards establishing new therapeutic treatments with higher efficacy for this population.

2.1 Functional Network Connectivity

Examination of FNC has been a growing topic of interest in the more recent years. Through the use of fMRI, research has been able to determine *in vivo* low frequency fluctuations in BOLD signals. This technique is high applicable to clinical research and diagnoses, has been used to characterize networks during resting-state and cognitive tasks, and is used to determine network changes in various disease states, including autism spectrum disorder, bipolar disorder, and schizophrenia [3]. Investigations of human patients with schizophrenia have been able to identify network disruptions that are linked to cognitive deficits. Research has found that schizophrenia patients have a higher number of errors and longer reaction times during working memory tasks and display spatially different fMRI activation within the dorsolateral prefrontal cortex (DLPFC) in comparison to the healthy individuals [36]. Furthermore, Potkin et al. (2009) similarly found that schizophrenia subjects display decreased accuracy and longer reaction times during the Sternberg Item Recognition Paradigm, a working memory task involving differing memory loads. Schizophrenia subjects display significantly different activation in the DLPFC than the normal controls, which is dependent upon memory load [39]. Kim et al. (2009) determined that during an auditory discrimination task, schizophrenia patients display irregularities in default-mode networks, many of which were in the DLPFC [34]. Cognitive deficits have

been explored within the schizophrenia population through various behavioral studies. Hanlon et al. (2006) discovered that patients with schizophrenia are impaired in the hidden-platform virtual water maze task (VWMT) [28]. These impairments were evident through diminished time spent in the correct target quadrant during probe trials and longer search paths in comparison to the normal controls. Garrity et al. (2007) also found disruptions in local spatial patterns and temporal frequency in the default mode network during behavioral tasks that required responding to salient stimuli [21]. Although components and networks can be identified through *in vivo* neuroimaging, these studies do not have the ability to identify neurobioloigcal mechanisms responsible for FNC alterations. Research has begun to study rats *in vivo* in order to establish translational work that will allow for the investigation of FNC and related neurobiological manipulations. Hutchinson et al. (2010) have been able to successfully scan anesthetized rats and analyze resting-state components through an ICA of whole-brain BOLD signals [29]. They were able to identify 12 independent resting state networks and found these networks to be similar to those found in humans at rest. Additionally, comparable default mode networks have been identified in rat and human brains [45]. This network includes the orbitofrontal cortex, cingulate gyrus (rats) or anterior cingulate cortex (humans), hippocampus, and posterior parietal cortex. Successful comparable fMRI scanning in human patients with schizophrenia and in rodent systems motivates exploration of FNC within an animal system that mimics schizophrenia-like symptoms.

2.2 N-methyl-D-aspartate (NMDA) Receptors

There are a number of approaches to modeling schizophrenia-like symptoms in animals, which include the use of transgenic animals [26], manipulations via lesions [32], and through the administration of NMDA antagonists [14,22,31]. Properly function-

ing neurotransmission through NMDA receptor requires binding of both glutamate and glycine in addition to partial membrane depolarization, which allows the release of the magnesium ion block. A lack of depolarization and/or blocking of one or both of the binding sites prevents the receptor from opening, which can affect the functioning of the entire neuron. Dysfunctional receptors can trigger non-optimal downstream effects, which have the potential to inhibit the entire system's ability to function properly. Injections of noncompetitive NMDA antagonists induce schizophrenia-like symptoms in healthy humans and animal models in addition to exacerbating symptoms in those who are already diagnosed with schizophrenia [7, 26, 35]. These findings support the theory that NMDA receptors have a fundamental role in the neuropathology of schizophrenia and have established a foundation for the NMDA receptor hypofunction hypothesis. This hypothesis states that the mechanisms responsible for the rise of schizophrenia-like symptoms are dysfunctional NMDA receptors, primarily on GABAergic interneurons. This dysfunction leads to an abundance of glutamate in the extracellular space causing a lack of excitation of GABAergic interneurons, which leads to a lack of inhibition on groups of various neurons receiving inputs from the dysfunctional GABAergic interneurons. The absence of inhibition of groups of neurons can disrupt the overall function of neuronal networks and could lead to downstream cognitive deficits. Due to the abundant evidence that manipulating NMDA receptors leads to schizophrenia-like symptoms, translational animal research has often used this as a model to mimic and explore this disease state. These models involved the administration of NMDA receptor antagonists, such as MK-801, ketamine, and phencyclidine (PCP). PCP is a noncompetitive NMDA receptor antagonist commonly utilized pharmaceutical drug in modeling schizophrenia. PCP blocks the activation of the receptor from within the receptor pore and exposure has been found to have lasting effects. on both presynaptic and postsynaptic structures [31]. Previous research has shown that chronic exposure to PCP decreases mRNA expression of GABAergic markers parvalbumin, calbindin, ErbB4 and GAD_{67}

and alters NMDA receptor subunits GluN2A and GluN2B [1, 4, 10, 11, 18, 48]. These mRNA expression deficits have been primarily identified in frontal cortex structures that are key to cognitive function and that have been highly associated with changes found in schizophrenia [10, 16]. Consistent findings of various markers being altered after assaulting a system with PCP has motivated researching mRNA expression to help verify this specific chronic PCP model as a valid model.

2.3 Behavioral Changes

Chronic and sub-chronic administration of PCP in animals also induce several behavioral changes, many of which mimic those found in the schizophrenia population. Abdul-Monim et al. (2006) found that sub-chronic administration of PCP (2mg/kg) significantly impeded correct responding during the reversal phase of operant learning [2]. Reversal learning in a spatial discriminant two-lever operant learning task was also disrupted by sub-chronic administrations of PCP at a dose of 1 mg/kg and 2 mg/kg [17]. Deficits in extradimensional set shifting using an attentional set shifting paradigm and sensorimotor gating through pre-pulse inhibition testing have also been consistently induced through the use of varying dosages of sub-chronic PCP administration [19, 23]. All of these behavioral alterations are analogous to cognitive deficits commonly found in schizophrenia patients [30].

The MWT is an experimental paradigm that explores learning and memory abilities and is dependent upon NMDA receptor function. Increases in GluN2A protein expression has been linked to the plasticity of spatial memory and was found to be pivotal for short term memory processing while GluN2B protein expression has been positively correlated with long-term memory processing [33]. Inversely, exposure to NMDA agonists, such as GLYX-13, has shown to promote learning and memory abilities in animals [12]. Furthermore, enhancement of GluN2B function has been

shown to enhance long-term memory performance in MWT [8]. Due to the role of NMDA receptors in learning and memory performance, MWT has been used to characterize and validate the use of NMDA antagonists in animals. PCP consistently impairs performance in spatial learning and memory and learning flexibility in the MWT [6, 26]. Due to the strong association between NMDA receptor manipulation and behavioral performance in MWT, we chose to use this paradigm to characterize how our PCP regimen manipulates spatial learning, memory, and behavioral flexibility. This behavioral task can help verify the validity of this PCP model and can assist in exploring the relationship between these behavioral outcomes and the cognitive deficits found in the schizophrenia population.

2.4 Innovation

Minimal research has explored the effects of PCP through *in vivo* scanning. For example, Gozzi et al. (2008) used pharmacological magnetic resonance imaging (phMRI) in order to examine the effects of an acute administration of PCP (0.5 mg/kg i.v.) and its interaction with D-serine and SSR504734 [27]. Barnes et al. (2015) found decreased cortical thickness and gray matter in rats exposed to PCP (5 mg/twice daily for 7 days) [5] yet no research has been undertaken to examine FNC changes in an animal system that has been manipulated by a low dose, sub-chronic model of PCP in order to mimic schizophrenia-like symptoms [16, 37]. Our research aims to characterize resting-state FNC through a sub-chronic, low-dose administration of PCP. We hope to identify components and networks that can be related to results from human schizophrenia fMRI research. Furthermore, we aim to validate mRNA and behavioral outcomes that are commonly associated with NMDA receptor manipulations and schizophrenia. This type of research could be a large step in validating animal models, which could be a stepping stone to other innovative

techniques in analyzing, diagnosing, and treating disease states that are associated with NMDA changes.

Chapter 3

Materials and Methods

3.1 Subjects

Forty male hooded Long Evan rats (Charles River Laboratories International, Inc.) weighing 340-400 grams at the beginning of treatment were housed in the Biomedical Research and Integrative NeuroImaging Center (BRaIN) animal research facility under a 12h/12h light/dark cycle (lights on at 7:00am). All animals were acclimated for 2 weeks before the start of the study and were pair-housed with a same-drug condition cage-mate in standard plastic cages with food and water available ad libitum. All animals were briefly anesthetized with isoflurane and ear notched. Rats were handled daily for one week prior to the beginning of behavioral testing and the start of injections. Rats were randomly assigned to the PCP treatment (n=20) or to the saline vehicle control treatment (n=20). Within the two drug treatment groups the animals were randomly assigned into 2 equally sized groups, one of which was scanned only on day 29 and other that was scanned on days 29 and 36 (PCP/scanned on day 29 only: n=10, saline/scanned on day 29 only: n=10, PCP/scanned on days 29 and 36: n=10, saline/scanned on days 29 and 36: n=10). All animals were treated

in accordance to the National Institutes of Health Guidelines for the Care and Use of Laboratory Animals. All experiments were approved by the Institutional Animal Care and Use Committee of the University of New Mexico Health Sciences Center.

3.2 Drugs

D-phencyclidine hydrochloride (PCP) was obtained from Sigma, dissolved in sterile Dulbecco's phosphate buffered saline solution (Sigma), and balanced at a pH of 7. After 1 day of training in the hidden platform MWT, PCP (2.58 mg/kg/injection) was administered to 20 rats through intraperitoneal (i.p.) injections. Sterile 0.9% saline solution (1 mL/kg) was administered as a vehicle control to 20 rats through i.p. injections. All animals received 14 injections over a 26 day period. Injections were given daily for the initial 5 consecutive days then for three days over each of the following three weeks. This resulted in rats receiving injections on days 1, 2, 3, 4, 5 (week 1), 8, 10, 12 (week 2), 15, 17, 19 (week 3), 22, 24, and 26 (week 4; see Figure 3.1).

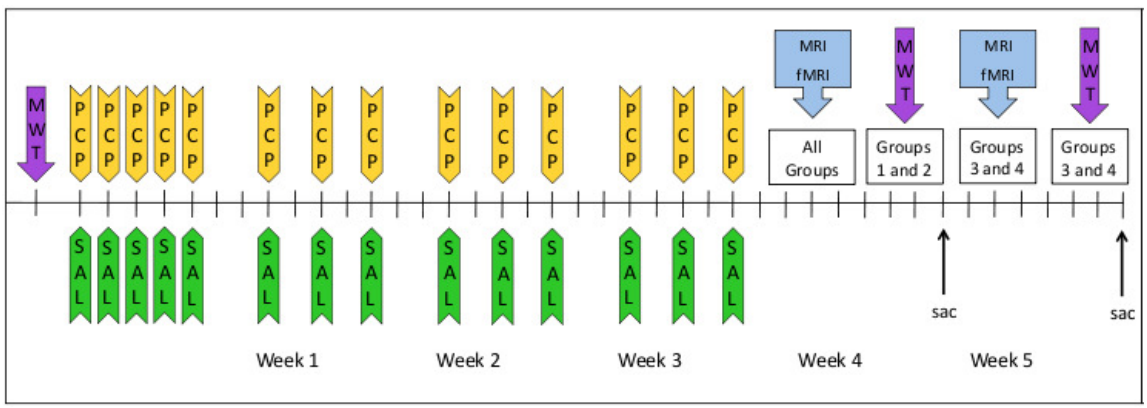

Figure 3.1: Timeline of sub-chronic sub-intermittent treatment of PCP or saline, fMRI scanning, behavioral testing, and tissue collection.

3.3 Behavioral Testing

3.3.1 Hidden Platform Morris Water Task (MWT)

A blue circular pool (74 cm deep, 175 cm diameter) was placed in the middle of the testing area and filled with water to a depth of ∼28 cm. The water was approximately 21-23^{o}C and was made opaque by the addition of nontoxic powered white paint. The pool was surrounded by two white-painted brick walls on the north and west sides and two gray fabric walls on the south and east side created by a portable partition (200 cm high, 500 cm wide). The platform (27 cm high, 16 cm wide, 16 cm length) was made of white PVC pipe and similar white materials. The top of the platform was covered in a metal wire grid to allow the animals to get on it with ease. It was placed in the pool in the middle of the north or south quadrant and was submerged under ∼1 cm of water. Different complex cues were hung on the walls nearby the northwest and south locations and a simple cue was located by the east. Additionally, there was a paper towel dispenser at the west location and a large gap between the white brick wall and the gray partition that may have served as distal cues for the animals. Behavior was recorded by an overhead camera which was attached to a video recording system. Videos were imported and digitized in order to track and analyze the animal's behaviors.

Pre-injection Training

All animals were ran through a total of 16 training trials and one probe trial the day before starting injections. This was done in order to establish a baseline of behavior before being introduced to any type of treatment or scanning. Pre-training allows for the comparison of how the animal behaved initially to how the animal behaved after receiving their treatment. Furthermore, allowing for a pre-training

period helps verify that any behavioral changes seen after the injection regiment are attributable to the treatment and helps eliminate the possible effects of non-specific learning deficits (e.g. initially learning how to swim, learning that there is a platform, learning not to engage in thigmotaxic search, and learning to search the open area). The platform was hidden 37 cm from the pool wall in the center of the north or south quadrant. Half of the animals were trained with the platform in the north quadrant and the other half in the south quadrant in order to account for possible location bias. Each animal was trained for four blocks consisting of four trials per block (total of 16 trials). In each of the blocks, the rat was released once in each of the equally spaced intermediate cardinal directions (northwest, northeast, southwest, and southeast) around the perimeter of the pool. The sequence of the release points was randomized within and between blocks. Once the animal was released, it had 60 seconds to find the hidden platform. The experimenter tracked the latency from the time the animal was released to the time that the animal's front paws touched the platform. If the animal did not find the platform within the allotted time, it would be guided to the platform by the experimenter and allowed to observe the surroundings for a few seconds before being brought back to its holding cage. Animals were tested in groups of three and were towel-dried in front of a heater after the first block and after the third block to help alleviate any possibility of hypothermia or exhaustion. After the completion of the training trials, the rats were tested in one no-platform probe trial. For the probe trial, the platform was removed from the pool and the animals were released in a novel location, either west or east. The rats were allowed to swim for 45 seconds before being removed from the pool and placed back in its holding cage. Searching behaviors were analyzed during this trial by examining how long they spent in the hidden platform quadrant and how many times they crossed the spot corresponding to the trained platform location. All trials were taped via an overhead camera. Video was digitized and transferred to a Mac workstation for the use of tracking software developed in our laboratory. The coordinates obtained from

the tracking software were used to obtain the dependent measures of interest, such as latency and swim path length to reach the platform location.

Post-scan Testing

On the day following the final scan, all animals were retested in the MWT. The post-scan test consisted of 1 probe trial, 8 retraining trials, a break of at least one hour, 4 retraining trials and 8 reversal trials. In the initial no-platform probe trial, each animal was released in the same novel location, either east or west, as they were released in the pre-treatment probe trial. The animals were allowed to swim for 45 seconds, removed from the pool by the experimenter, and placed back in their home cage. The platform was placed in the original training location, either north or south, and the animals were retrained for 2 blocks (4 trials per block). Again, each block consisted of the rat being released once in each of the equally spaced intermediate cardinal directions (northwest, northeast, southwest, and southeast) around the perimeter of the pool. The sequence of the release points was randomized within and between blocks. Just as in pre-training, once the animal was released it had 60 seconds to find the hidden platform. The experimenter tracked the latency from the time the animal was released to the time that the animal's front paws touched the platform. If the animal did not find the platform within the allotted time, it would be guided to the platform by the experimenter and allowed to observe the surrounding area for a few seconds before being brought back to its holding cage. After the initial retraining session was complete, the animal was towel-dried in front of a heater before being placed back in its home cage in the colony room. The animal was given a break of at least 1 hour in its home cage between the two bouts of testing. The second half of testing examined the flexibility of the learning within the different treatment and scan time groups. Rats were given 1 block of 4 trials of retraining where the platform was in the original training location. Following this retraining

session, rats were tested in a reversal paradigm where the platform was moved to the opposite location in the pool. If the animals were trained with the platform in the north quadrant, the platform was moved to the south quadrant and vice versa. Rats were then released in one of the four intermediate cardinal locations and allowed to search for the platform for 60 seconds, just as in the retraining trials. Testing and latency recordings were conducted and tracked in the same manner described in the retraining section above. After the animals completed the reversal sessions, the rats were sacrificed and tissue was collected for mRNA expression analysis.

3.4 fMRI Scanning

On day 29, three days after the completion of the sub-chronic treatment administration, all animals (weighing 392-559g at the time of scanning, mean weight = 445.64g) were scanned in the 4.7T Bruker Biospin MRI Scanner (BRaIN MR Imaging Core). Additionally, a subset of animals (weighing 400-542g at the time of scanning, mean weight = 469.65g) were rescanned on day 36, allowing for a washout period of 7 days from the initial scan time point. In preparation for imaging animals were individually, rapidly anesthetized with isoflurane, placed in the animal holder/MRI probe apparatus, and positioned inside the magnet with the head stabilized in a fixed location within the imaging coil. Anesthesia was maintained with 2.5% isoflurane carried by O_2 (1L/minute) through a close fitting snout mask. Body temperature, respiration rate, CO_2, and O_2 levels were continuously monitored and recorded throughout the scanning sessions. RARE-8 T1 image sequences were collected for co-registration with the following parameters: slice thickness=1mm, TE=56ms, flip angle=180^o, FOV=3.84x3.84 cm^2, matrix=256x256. The anatomical scan included shimming and allowed for the isoflurane concentration and global hemodynamics to stabilize prior to acquiring fMRI images. Resting state fMRI BOLD data were collected

after the anatomical scan with an echo-planar imaging (EPI) acquisition sequence with the following parameters: 26 1 mm slices, TR=2s, TE=21ms, flip angle=90^o, FOV=3.84x3.84 cm^2, matrix=64x64. Finally, arterial spin labeling (ASL) image data were collected to address blood perfusion with the following parameters: 1 mm slices, 44 averages, TR=16s, TE=45.99ms, flip angle=180^o, FOV=3.84x3.84 cm^2, matrix=128x128.

3.5 Quantitative Real-Time PCR (qRT-PCR)

Upon the completion of the Morris water task post-scan session, rats were anesthetized using isoflurane and decapitated. Tissue punches from the medial frontal cortex, ventral frontal cortex, M1/M2 region, and the parietal cortex in addition to the whole cerebellum and bilateral hippocampi were extracted and placed into individual 1.5mL RNAse-free tubes. The tissue samples were frozen on dry ice and stored at -80^{o}C. qRT-PCR analysis were conducted as described previously in Bullock et al. (2008) and Bullock et al. (2009) [10,11]. Tissue samples were homogenized using a Polytron homogenizer (Brinkmann Instruments, Inc.; Westbury, NY). Total RNA was isolated using an RNeasy mini kit (Qiagen). cDNA was synthesized from a portion of the total RNA using Superscript II reverse transcriptase (Life Technologies) in accordance with the manufacturer's protocol. Exon spanning primer pairs specific to GABAergic markers parvalbumin, calbindin, ErbB4, and GAD_{67} and NMDA receptor subunits GluN2A and GluN2B were designed by using Primer Express 3.0 (Life Technologies) and validated through the use of NCBI primerBLAST software. All RT-PCR reactions were ran in an Applied Biosystems 7000 machine. Gene expression levels for all tissue samples were measured using SYBR® Green (Life Technologies). Expression levels for the genes of interest were normalized against those of β-actin. Primer dimerization were examined by dissociation curve analyses.

3.6 Analysis

All image preprocessing was conducted in SPM8 (www.fil.ion.ucl.ac.uk/spm). EPI image sequences were realigned, spatially normalized to a template brain [42] corresponding to the atlas of Paxinos and Watson with a final voxel size of 0.2mm^3, and smoothed (0.8mm kernel). FNC data were assessed using a group (ICA) approach through the implementation of the Group ICA of fMRI Toolbox (GIFT, http://mialab.mrn.org/software/gift/index.html). We determined the between component correlation coefficients for each animal, estimated 40 components, and excluded artifactual components based on visual inspection. Group-wise differences were analyzed in component spectra and functional connectivity (cross-correlations). Expression of mRNA for parvalbumin, calbindin, ErbB4, GAD_{67}, NR2A, and NR2B were normalized against expressions of β-actin using $2^{-\Delta\Delta CT}$ method [41]. Primer dimerization were examined by dissociation curve analyses. Latencies and path lengths for each training trial were quantified for each rat. Different repeated measures analysis of variances (ANOVA) were conducted for the pre- treatment and the two post-scanning time points. Additionally, an ANOVA was conducted in order to compare the averaged latencies and path lengths of the re-training block and the reversal blocks.

Chapter 4

Results

4.1 Functional Network Connectivity (FNC)

4.1.1 Orientation To The Presentation Of The FNC Results

An explanation of the following results section was deemed necessary due to the high density of the data. This section of the document has been formed in order to orient the reader to the organization of the FNC dataset. The results section begins by quantitatively and qualitatively describing the components observed in this study. These components will be used throughout the rest of the analyses in order to assess connectivity. An overall FNC matrix collapsed across treatment groups and time points will be presented. The rest of the connectivity results will be described according to the associated time that the scan occurred. All data from day 29 will be described followed by all of the data from day 36. Within each time point the following organizational tier will be applied. First, there will be qualitative and quantitative descriptions and figures of the treatment specific (saline and PCP) FNC matrices. Additionally, descriptions of the qualitative differences between the

treatment groups will be described. Statistical analysis (t-tests) on the effects of the treatment will be presented followed by the details of the significant differences. These simple analyses were conducted in order to assess the effect of exposure to PCP versus saline. Following the results from the individual scan time points, there will be qualitative and quantitative descriptions of the effect of the one-week wash out period. The statistical analyses (t-tests) will be presented followed by the details of the significant differences. The reader is encouraged to reference figures (4.1-4.10) while reading the results section in order to gain a comprehensive understanding of the FNC data.

4.1.2 Components

A total of 21 non-artifactual components were retained from the initial set of 40 components throughout the striatum, thalamus, cortex, hippocampal, midbrain and cerebellum (see Figure 4.1).

Specifically, three striatal (St1-St3), four hippocampal (H1-H4), ten cortical (Cx1-Cx10), one thalamic (T1), one cerebellar (Cb1), and two midbrain (Mb1-Mb2) components were retained for the group component analysis using the FNC toolbox within the Group ICA of fMRI (GIFT) toolbox. The iq (stability) for these components ranged between 0.91-0.97 with a mean of 0.95. Artifactual components were excluded based on visual inspection of the spatial location and distribution of the component. In the figures, the components are labeled according to the brain region associated with the peak and organized anterior to posterior within each brain region.

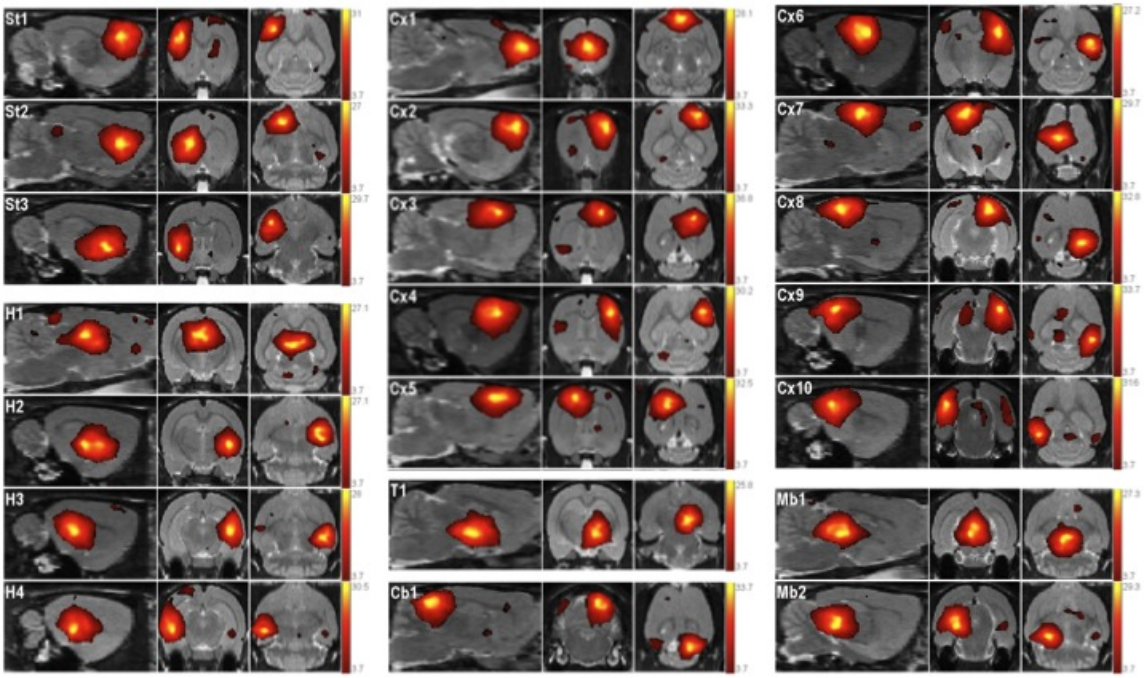

Figure 4.1: Twenty-one non-artifactual components identified and used throughout functional network connectivity and spectral time course analyses. Component t-map images are composed of sagittal, coronal, and transverse views with a threshold of 3.7. Components are organized anterior to posterior within brain regions and based off of the peak t-value indicated by the yellow coloring.

4.1.3 Overall Functional Network Connectivity

Throughout all analyses relationships were deemed significant at $p<0.005$ (black dots) or $p<0.00025$ (white dots). When collapsing across both treatment groups and both time points, 154 relationships out of 210 pair-wise comparisons were found to be significant (see Figure 4.2).

Most relationships were found to be significant at $p<0.00025$. Specifically, the 154 significant correlations were composed of 129 relationships that were significant at $p<0.00025$ and 25 relationships that were significant at $p<0.005$. All major brain regions were significantly correlated within and between all other brain regions in

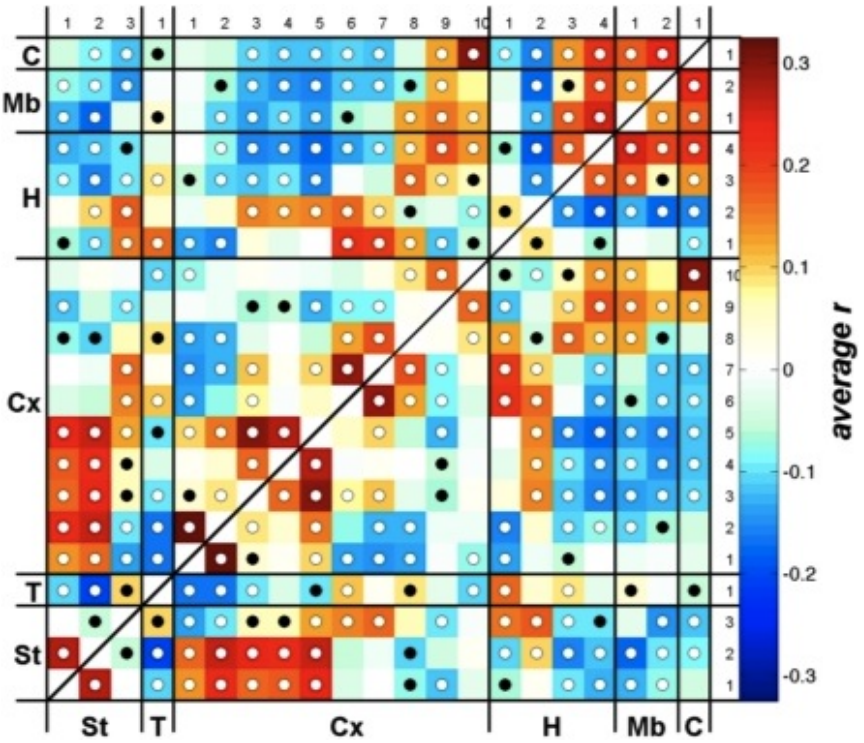

Figure 4.2: Overall correlations matrix demonstrates which components are significantly different than zero when components are collapsed across both treatment conditions.

some way. There were no regions that completely lacked a significant relationship with another brain region. Of the 154 significant relationships 72 were positive correlations and 82 were negative correlations. Positive correlations were identified in striatal-anterior cortical, posterior striatal-anterior hippocampal, thalamic-mid-cortical, thalamic-hippocampal, thalamic-midbrain, posterior hippocampal, posterior cortical-midbrain, posterior cortical-cerebellar, posterior hippocampal-midbrain, posterior hippocampal-cerebellar, and midbrain-cerebellar component relationships. Negative correlations were identified in striatal-thalamic, striatal-posterior cortical, striatal-posterior hippocampal, striatal-midbrain, striatal-cerebellar, thalamic-anterior cortical, thalamic-cerebellar, anterior cortical-midbrain, anterior cortical-cerebellar, anterior hippocampal-midbrain, and anterior hippocampal-cerebellar com-

ponent relationships. Overall, midbrain and cerebellar components tend to follow the same directional trends and components that occur spatially close to one another tend to be positively correlated and negative correlated to components that are spatially distant.

4.1.4 FNC on Day 29 - Saline Exposed Animals

All animals received an fMRI scan on day 29, three days after the final injection. At this time point saline exposed animals displayed a total of 89 significant relationships out of 210 pair-wise comparisons (see Figure 4.3).

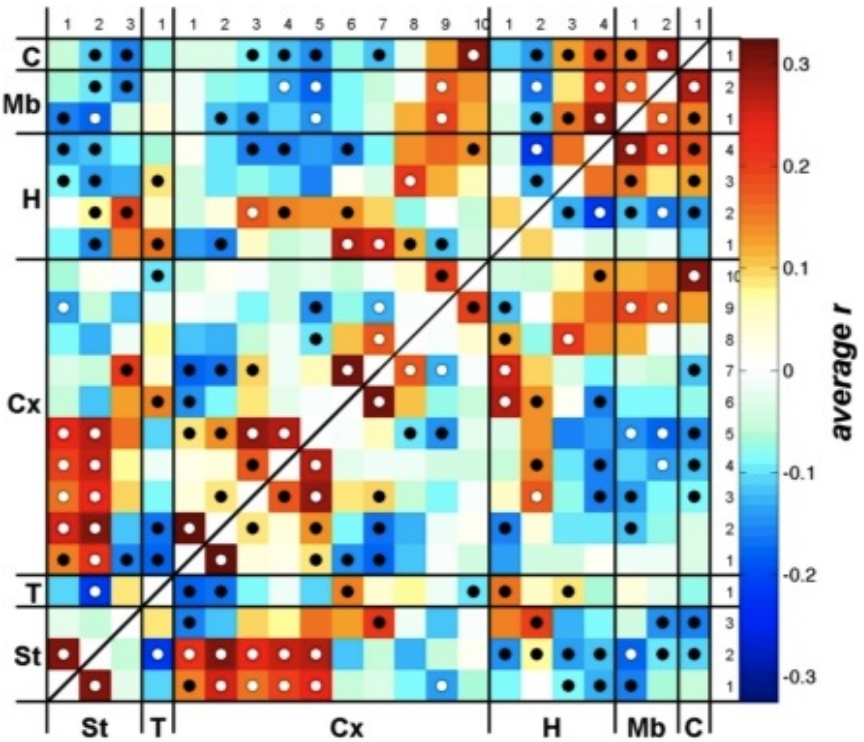

Figure 4.3: Day 29 FNC for saline exposed animals - correlations matrix demonstrates which components are significantly different than zero. White dots indicate significance at $p<0.00025$. Black dots indicate significance at $p<0.005$.

A majority of the relationships were significant at $p<0.005$. Specifically, the

89 significant correlations were composed of 54 relationships that were significant at $p<0.005$ and 35 relationships that were significant at $p<0.00025$. Of the 89 significant relationships 47 were positive correlations and 42 were negative correlations. Most positive correlations were found in striatal-anterior cortical and midbrain-cerebellar relationships and scattered throughout cortical-cortical, cortical-anterior hippocampal, posterior cortical-midbrain, posterior hippocampal-midbrain, and posterior hippocampal-cerebellar component relationships. Negative correlations were primarily found in striatal-posterior hippocampal, striatal-midbrain, striatal-cerebellar, anterior cortical-midbrain, anterior cortical-cerebellar, anterior hippocampal-midbrain, and anterior hippocampal-cerebellar and scattered throughout anterior cortical-posterior cortical, cortical-hippocampal, and within hippocampal component relationships.

4.1.5 FNC on Day 29 - PCP Exposed Animals

On day 29, PCP exposed animals showed similar trends as the saline exposed animals. The PCP exposed animals displayed a total of 86 significant relationships (see Figure 4.4).

A majority of the relationships were significant at $p<0.005$. Specifically, the 86 significant correlations were composed of 56 correlations that were significant at $p<0.005$ and 30 correlations that were significant at $p<0.00025$. Of the 86 significant relationships 46 were positive correlations and 40 were negative correlations. Most correlations found in the PCP exposed animals followed a similar trend to those found in the saline exposed animals. The biggest differences are the decreased number of significant relationships in the striatal-cerebellar, striatal-hippocampal, thalamic-hippocampal, thalamic-cortical, and cortical-cortical component correlations. Additionally, there was an increased number of significant correlations in

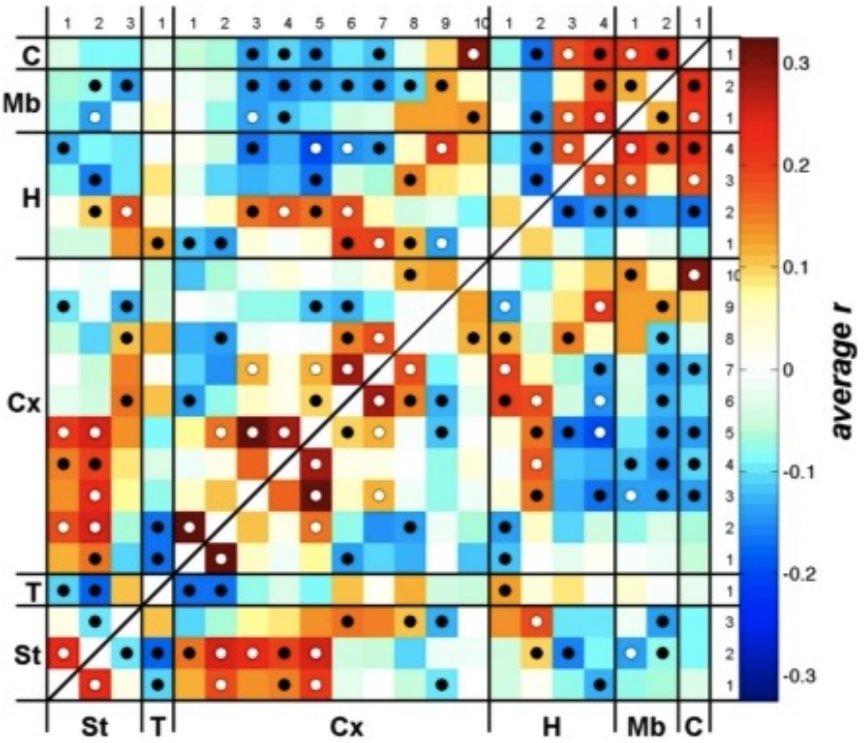

Figure 4.4: Day 29 FNC for PCP exposed animals - correlations matrix demonstrates which components are significantly different than zero.White dots indicate significance at p<0.00025. Black dots indicate significance at p<0.005.

the PCP exposed animals in striatal-thalamic, striatal-striatal, cortical-hippocampal, and cortical-midbrain component relationships.

4.1.6 FNC - Statistical Analysis of Treatment Effects on Day 29

Two-sample t-tests where the saline FNC matrix was subtracted from the PCP FNC matrix (PCP-Sal) revealed 4 significant differences between the treatment groups (see Figure 4.5).

Three of the 4 significant differences resulted from the PCP animals displaying an

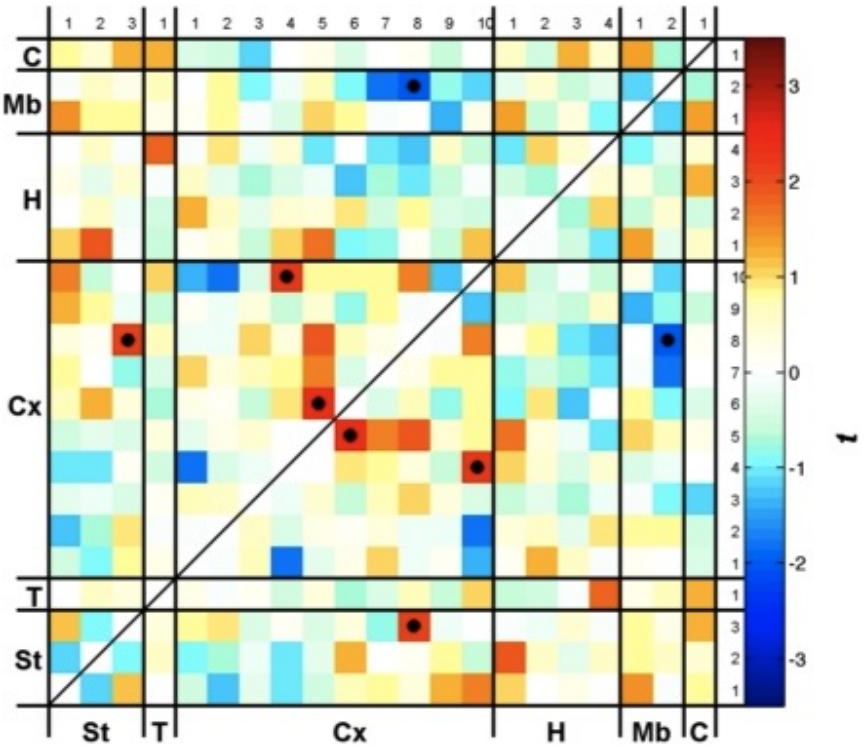

Figure 4.5: T-test conducted to determine treatment effects occurring on day 29. The saline data were subtracted from the PCP data (PCP-Sal) in order to determine the differences between the treatment groups. Black dots indicate significance at $p<0.005$.

increased positive correlation as indicated by the red coloring of the significant boxes. These occurred in the striatal(3)-cortical(8), cortical(5)-cortical(6), and cortical(4)-cortical(10) component relationships. Upon further investigation, these significant differences arose from the saline animals displaying negative correlations and the PCP animals displaying positive correlations in these specific relationships. The final significant relationship was between the midbrain (2) and the cortex (8). This negative correlation was driven from the saline group displaying a correlation of 0 and the PCP group displaying a significant negative correlation.

4.1.7 FNC on Day 36 - Saline Exposed Animals

Half of the animals in each treatment group received an fMRI scan on day 36, ten days after the final injection. At this time point saline exposed animals displayed a total of 10 significant relationships, which was a large decrease from the initial 89 significant correlations seen at day 29 (see Figure 4.6).

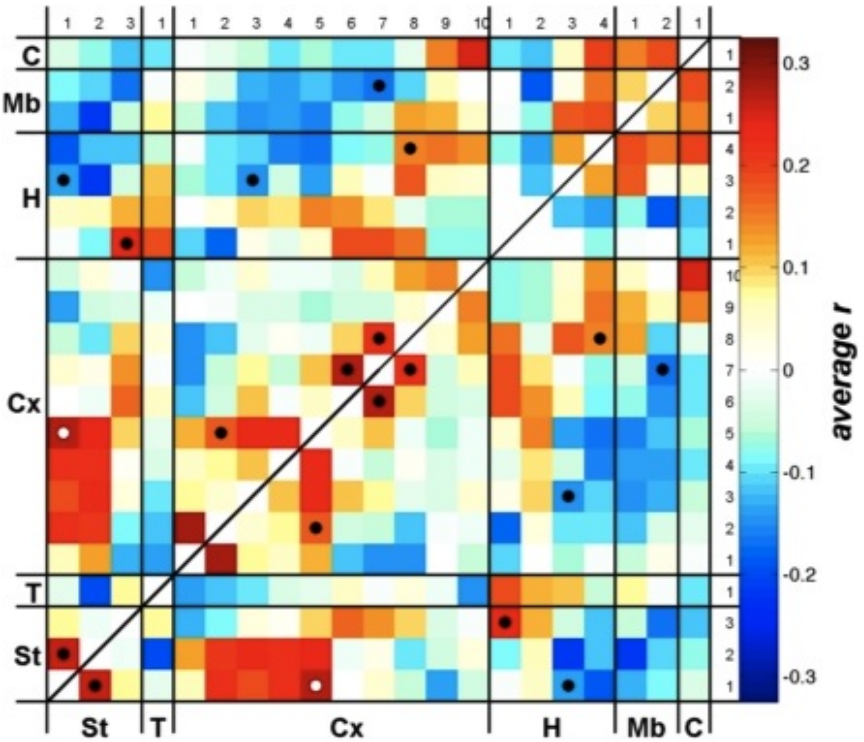

Figure 4.6: Day 36 FNC for saline exposed animals - correlations matrix demonstrates which components are significantly different than zero. White dots indicate significance at $p<0.00025$. Black dots indicate significance at $p<0.005$.

A majority of the relationships were significant at $p<0.005$. Specifically, nine of the ten significant correlations were significant at $p<0.005$. Of the 10 significant relationships 7 were positive correlations and 3 were negative correlations. The positive correlations were found within striatal, cortical, and hippocampal relationships and between striatal-cortical and striatal-hippocampal component relationships. Neg-

ative correlations were found between striatal-hippocampal, cortical-hippocampal, and cortical-midbrain component relationships.

4.1.8 FNC on Day 36 - PCP Exposed Animals

On day 36, PCP exposed animals showed an increased number of significant relationships compared to the saline exposed animals. The PCP exposed animals displayed a total of 40 significant relationships (see Figure 4.7).

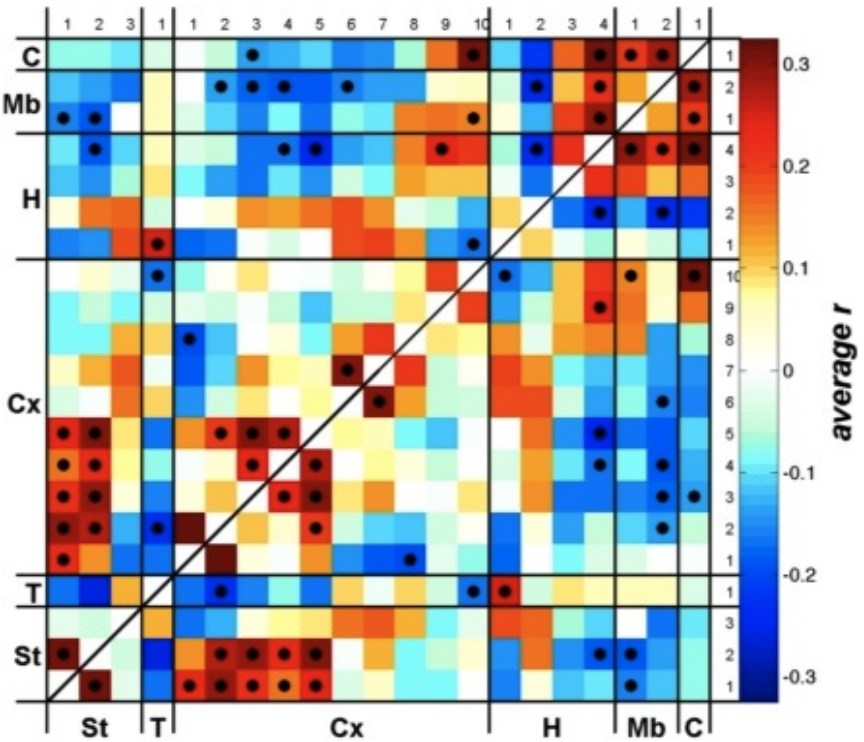

Figure 4.7: Day 36 FNC for PCP exposed animals - correlations matrix demonstrates which components are significantly different than zero. White dots indicate significance at $p<0.00025$. Black dots indicate significance at $p<0.005$.

All 40 of the relationships were significant at $p<0.005$. Of the 40 significant relationships 24 were positive correlations and 16 were negative correlations. Most of the

significant trends found in the saline exposed animals were also found in the PCP exposed animals. The was an increase in positive correlations in striatal-cortical, cortical-cortical, thalamic-hippocampal, cortical-hippocampal, midbrain-cerebellar, hippocampal-midbrain, cortical-midbrain, and cortical-cerebellar component relationships in the PCP exposed animals compared to the saline exposed animals. The PCP exposed animals also displayed an increase in negative relationships in thalamic-cortical, cortical-cortical, striatal-hippocampal, striatal-midbrain, cortical-hippocampal, cortical-midbrain, cortical-cerebellar, hippocampal-hippocampal, and hippocampal-midbrain component relationships.

4.1.9 FNC - Statistical Analysis of Treatment Effects on Day 36

Similar to the data found in the initial scan on day 29, two-sample t-tests where the saline FNC matrix was subtracted from the PCP FNC matrix (PCP-Sal) revealed 4 significant differences between the treatment groups (see Figure 4.8).

All 4 of the significant differences resulted from the PCP animals displaying an increased negative correlation as indicated by the blue coloring of the significant boxes. These occurred in the striatal(1)-striatal(3), striatal(1)-hippocampal(1), thalamic(1)-hippocampal(2), and cortical(2)-midbrain(2) component relationships. Upon further investigation, 2 of these significant differences arose from the saline animals displaying positive correlations and the PCP animals displaying negative correlations in the striatal(1)-striatal(3) and thalamic(1)-hippocampal(2) component relationships. The additional 2 significant relationships, striatal(1)-hippocampal(1) and cortical(2)-midbrain(2) were driven from the saline group displaying a negative correlation and the PCP group displaying an increased negative correlation. Unlike the t-tests conducted at the day 29 time period, the t-tests conducted on day 36 re-

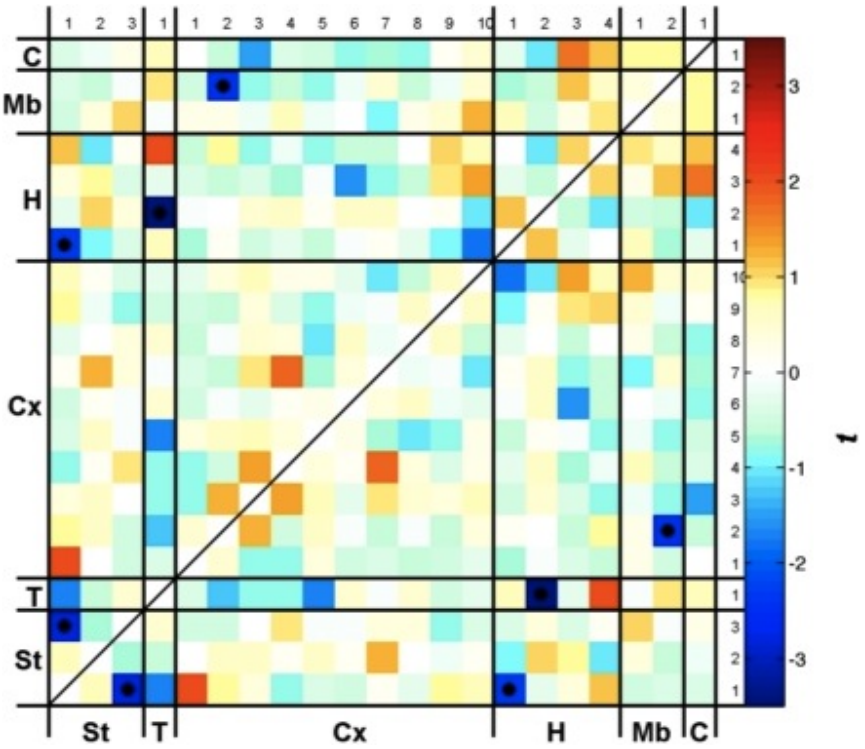

Figure 4.8: T-test conducted to determine treatment effects occurring on day 36. The saline data were subtracted from the PCP data (PCP-Sal) in order to determine the differences between the treatment groups. Black dots indicate significance at $p<0.005$.

sulted in mostly negative t-values (Sal>PCP). The total number of negative t-values increased and positive t-values decreased on day 36 when compared to day 29.

4.1.10 FNC - Statistical Analysis of the Cessation Period on Saline Exposed Animals

Two-sample t-tests where the day 36 data were subtracted from the day 29 data (Day 29-Day 36) revealed 4 significant differences between the scan time points (see Figure 4.9).

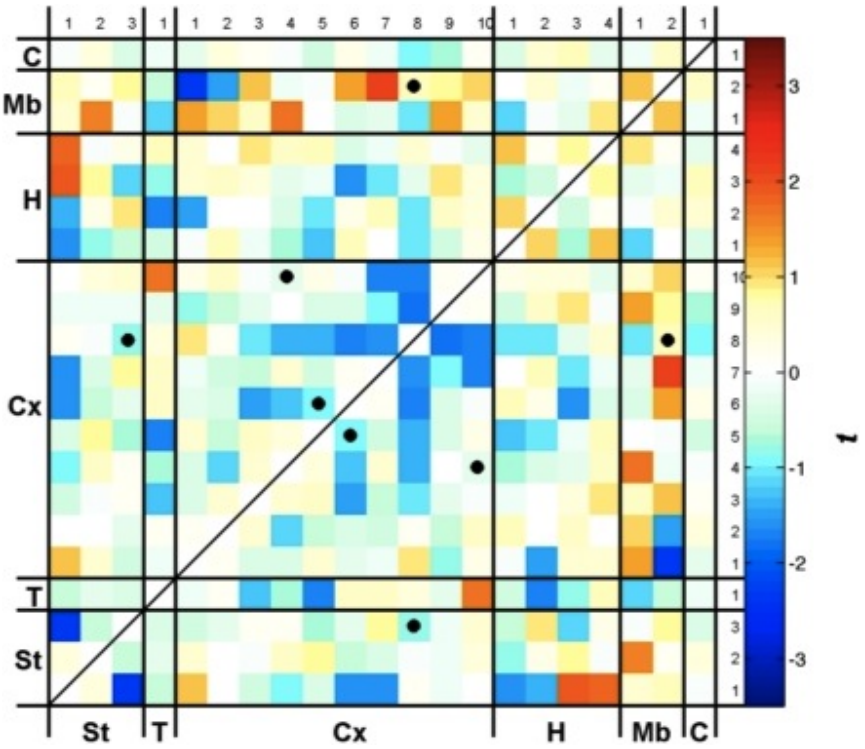

Figure 4.9: T-tests conducted to determine the effects of the 1 week washout period in the saline exposed rats. The data from day 36 were subtracted from the data from day 29 (Day 29-Day 36) in order to determine the differences between the two scan time points. Black dots indicate significance at $p<0.005$.

Three of the four significant differences resulted from the data from day 29 displaying an increased negative correlation as indicated by the blue coloring of the significant boxes (Day 36>Day 29). These occurred in the striatal(3)-cortical(8), cortical(5)-cortical(6), and cortical(4)-cortical(10) component relationships. Upon further investigation, the significant differences between striatal(3)-cortical(8) and cortical(5)-cortical(6) component relationships arose from the day 29 correlation being around 0 and the day 36 correlation being negative. The additional negative t-value found in the cortical(4)-cortical(10) component relationship was driven by the day 29 data being more negative than the day 36 data. The final significant relationship was between the midbrain (2) and the cortex (8). This positive correlation

was driven from the day 29 data displaying a positive correlation and the day 36 data displaying a negative correlation.

4.1.11 FNC - Statistical Analysis of the Cessation Period on PCP Exposed Animals

Again, two-sample t-tests where the day 36 data were subtracted from the day 29 data (Day 29-Day 36) revealed 4 significant differences between the scan time points (see Figure 4.10).

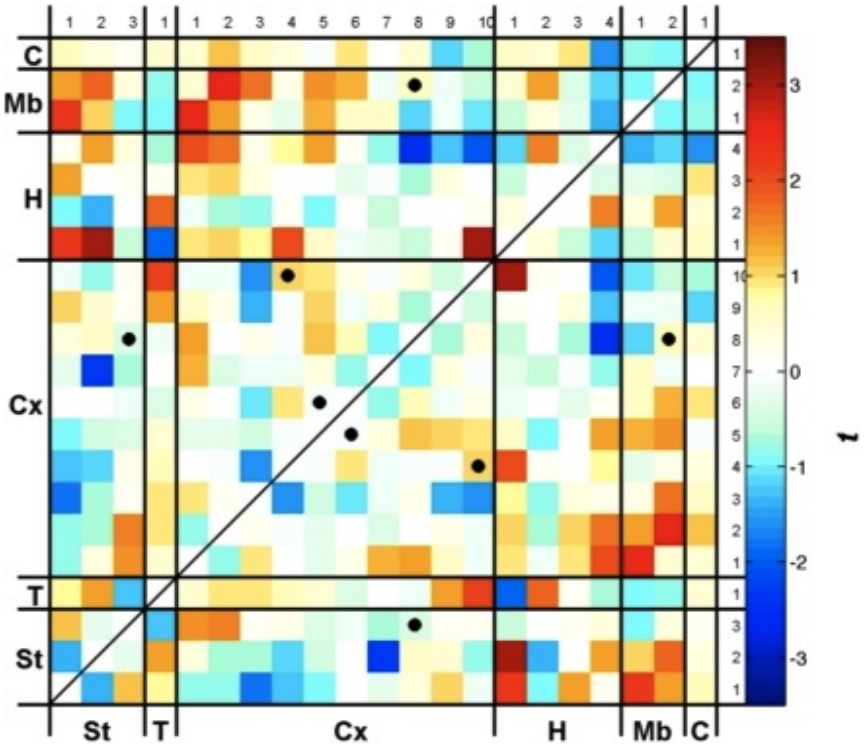

Figure 4.10: T-tests conducted to determine the effects of the 1 week washout period in the PCP exposed rats. The data from day 36 were subtracted from the data from day 29 (Day 29-Day 36) in order to determine the differences between the two scan time points. Black dots indicate significance at $p<0.005$.

Three of the four significant differences resulted from the data from day 29 dis-

playing an increased positive correlation as indicated by the yellow coloring of the significant boxes (Day 29>Day 36). These occurred in the midbrain(2)-cortical(8), cortical(5)-cortical(6), and cortical(4)-cortical(10) component relationships. Furthermore, the significant difference between the midbrain(2) and the cortical(8) component was driven from the day 29 correlation being negative and the day 36 correlation being a stronger negative correlation. The cortical(4)-cortical(10) component relationship was driven by the day 29 data being positive and the day 36 data being approximately 0. The final positive significant relationship was between the cortical(5)-cortical(6) components. This positive correlation was driven from the day 29 data displaying a stronger positive correlation than the day 36 data. Inversely, the fourth significant difference that occurred between the striatal(3)-cortical(8) components was negative and arose from the day 36 data displaying a stronger positive correlation than the day 29 data.

4.2 Spectral Power Analyses

4.2.1 Orientation To The Presentation Of The Spectral Results

An explanation of the following results section was also deemed necessary due to the high density of the data and has been formed in order to orient the reader to the organization of the spectral dataset. In regards to the figures, the components listed above the FNC section are ordered along the Y axis and the spectral bins are ordered along the X axis. The spectral data are organized into 0.04 Hz bins for purposes of simplicity. The data begins with the presentation of two-way analysis of variance (ANOVA) results that investigate significant interactions, main effects of treatment, and main effects of time point. Next, t-tests for the overall treatment

effect (PCP-Sal) and the overall effect of the cessation period (Day 29-Day 36) will be described. Additionally, t-tests assessing the treatment effects on the day 29 and day 36 will be presented. The reader is encouraged to reference Figures 4.11-4.13 while reading the results section in order to gain a comprehensive understanding of the spectral power data.

4.2.2 Spectral Power - ANOVA Interactions

A total of 4 significant interactions (treatment X time) were observed (see Figure 4.11 A). The midbrain component 1 was significant (Sal>PCP, Day 29>Day 36) in the 0.20-0.24 Hz range at $p<0.05$. The additional significant interactions were identified in the hippocampus. Hippocampal components 1 and 2 were significant in the 0.16-0.20 Hz range at $p<0.05$. Significance in hippocampal component 1 was driven by Sal>PCP and Day 36>Day 29 while significance in hippocampal component 2 was driven by Sal<PCP and Day 29<Day 36. Additionally, hippocampal component 3 was significant in the 0.08-0.12 Hz range at $p<0.05/6$. This result was due to Sal>PCP and Day 36>Day 29. The details of the results and further t-tests were conducted below.

4.2.3 Spectral Power - ANOVA Treatment Main Effect

ANOVAs yielded a total of 19 significant treatment main effects throughout the components (see Figure 4.11 B). These main effects were comprised of 12 effects that were significant at $p<0.05$ and 7 effects that were significant at $p<0.05/6$. Most of the A total of 7 effects were significant in the 0.00-0.04 Hz frequency range and were found in the midbrain (2), hippocampus (2, 3, and 4), cortex (2 and 5), and the striatum (2). Cortical component 3 was significant at 0.08-0.12 Hz, cortical component 4 and hippocampal component 3 were significant at 0.12-0.16 Hz, and cortical component

5 was significant at 0.16-0.20 Hz. Finally, 8 treatment main effects were significant at 0.20-0.24 Hz and were found in the cerebellum (1), hippocampus (2), cortex (1, 2, 4, and 5), thalamus (1), and the striatum (1). The details and further t-tests were conducted below.

4.2.4 Spectral Power - ANOVA Time Point Main Effect

ANOVAs resulted in 2 significant main effects ($p<0.05$) of the time point (see Figure 4.11 C). These main effects occurred in the striatum (3) and the midbrain (2). The striatum component was significant in the 0.16-0.20 Hz frequency range and the midbrain component was significant in the lowest frequency range of 0.00-0.04 Hz. Both striatum and midbrain significances were driven by Day 36>Day 29. Additional t-tests and details are described below.

4.2.5 Spectral Power - Statistical Analyses of Treatment Effects

Two-sample t-tests were conducted on all of the scans in order to determine the effects of the treatment on spectral power (see Figure 4.12A). These analyses were collapsed across scan time points and were conducted by subtracting all of the saline data from the PCP data (PCP-Sal). Overall, all of the components consistently displayed a stronger power in the PCP exposed animals (PCP>Sal) for the highest frequency bin of 0.20-0.24 Hz. As the power decreases, the t-values become more negative for almost all of the components. This results in the lowest frequency bins (0.00-0.04, 0.04-0.08, and 0.08-0.12) being comprised primarily of greater power in the saline exposed animals (Sal>PCP). Specifically, the treatment analysis resulted in a total of 17 significant differences ($p<0.05$ or $p<0.05/6$), 9 positive and 8 negative results.

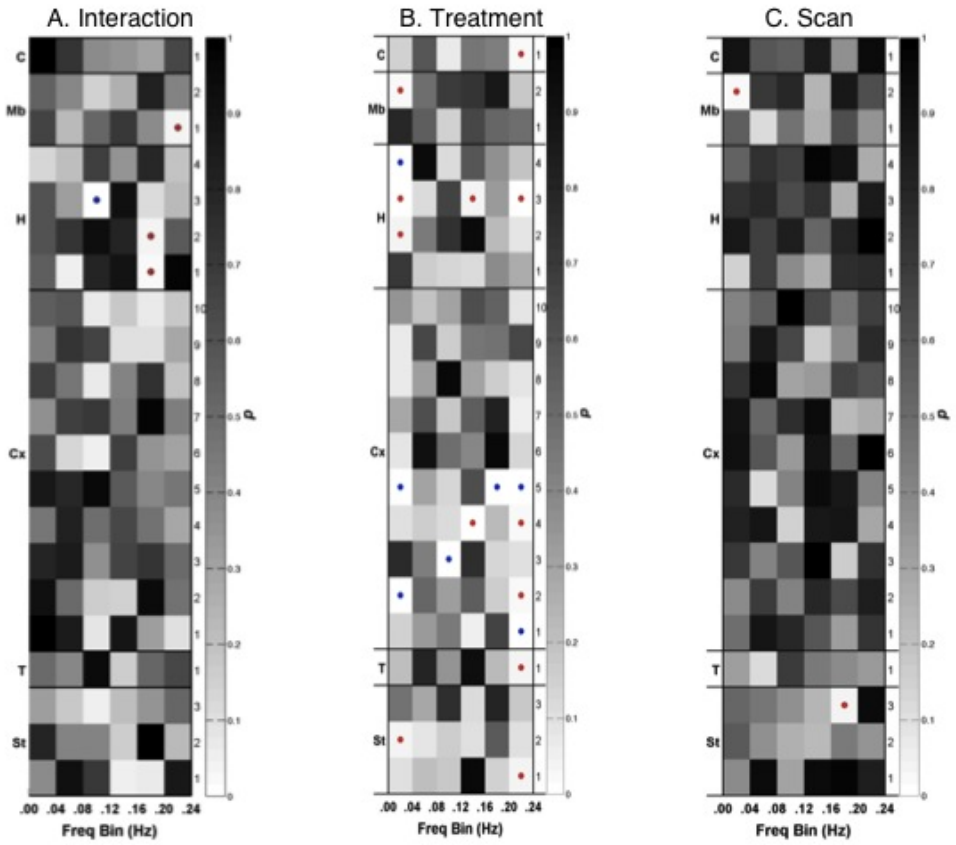

Figure 4.11: ANOVA omnibus p-value maps conducted on spectral power. The separate figures indicate significant (A) interactions, (B) the main effects of treatment, and (C) the main effects of the time point. Red dots indicate significance at $p<0.05$ and blue dots indicate significance at $p<0.05/6$.

PCP exposed animals displayed greater power in seven out of nine significant results (PCP>Sal). These effects occurred in the 0.20-0.24 Hz frequency and incorporated the striatum (1), thalamic (1), cortical (1, 5, and 7), hippocampal (3) and cerebellar (1) components. The PCP rats had significantly greater power in cortical component 5 at 0.16-0.20 Hz and in cortical component 4 at 0.12-0.16 Hz. The saline exposed animals displayed greater power (Sal>PCP) in 2 components at 0.12-0.16 Hz, 1 component at 0.08-0.012 Hz, and 5 components at 0.00-0.04 Hz. The significant effects at the 0.12-0.16 Hz frequency occurred in the cortical (1) and hippocampal

(3) components. The significant difference at 0.08-0.12 Hz occurred in the cortical 3 component. The majority of the effects occurred at 0.00-0.04 Hz and were identified in the striatal (2), cortical (2 and 5), hippocampal (4), and midbrain (2) components.

4.2.6 Spectral Power - Statistical Analysis of Cessation Period Effects

An examination of the cessation period was completed through two-sample t-tests, which were conduct on all of the animals that received 2 scans (n=20) regardless of treatment in order to determine the effects of the 1 week cessation period on spectral power (see Figure 4.12B). These analyses were collapsed across treatment and were conducted by subtracting all of the day 36 data from the day 29 data (Day 29-Day 36). There was a mix of increases (Day 29>Day 36) and decreases (Day 36>Day 29) in spectral power trending throughout the entire analysis, but, similarly to the treatment effect, there was a trend towards greater power in the Day 29 data in the highest frequency bin, 0.20-0.24 Hz and a trend towards greater power in the Day 36 data in the lower frequency bins, 0.00-0.04 and 0.04-0.08 Hz. Specifically, the time point analysis resulted in 1 significant difference ($p<0.05$). This significant result found in the midbrain (2) was due to the Day 36 data having greater power (Day 36>Day 29) and occurred in the lowest frequency bin, 0.00-0.04 Hz.

4.2.7 Spectral Power - Statistical Analyses of Treatment Effects on Day 29

An examination of the effects of treatment on spectral power was conducted on the entire group of scans from the day 29 time point (see Figure 4.13A). These analyses address the treatment effects that occurred 3 days following the final injection. The

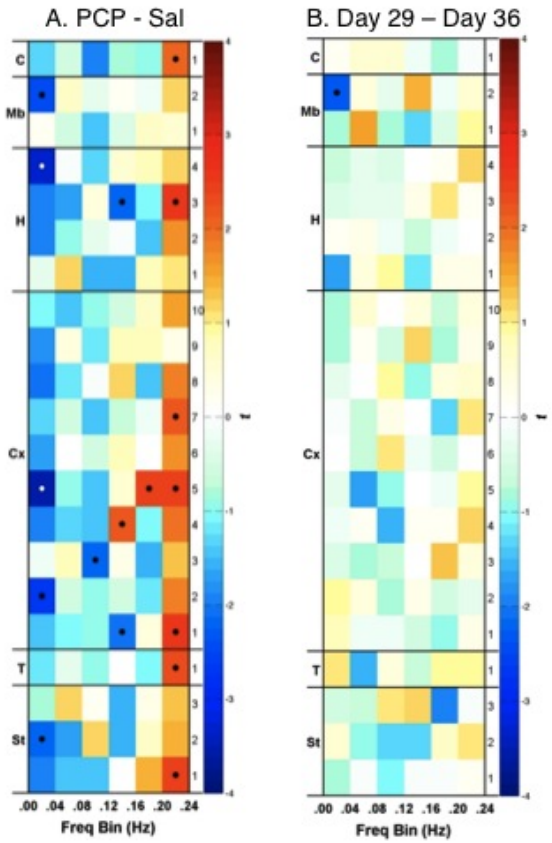

Figure 4.12: T-tests conducted to determine the effects of the treatment (A. PCP-Sal) and the 1 week washout period (B. Day 29-Day36). Black dots indicate significance at $p<0.05$ and white dots indicate significance at $p<0.05/6$.

results were completed by subtracting the saline data from the PCP data (PCP-Sal). Similarly to the data investigating time effects, there was a mix of positive and negative trends throughout the results. Again, there was a high prevalence of there being greater power in the PCP rats (PCP>Sal) in the highest frequency bin (0.20-0.24) and there being greater power in the saline rats (Sal>PCP) in the two lowest frequency bins (0.00-0.04 and 0.04-0.08). The treatment analysis on day 29 resulted in a total of 5 significant differences ($p<0.05$). Four out of the five significant results were due to an increase in spectral power in the PCP exposed animals compared to the saline exposed animals. Three of the increases occurred in the 0.16-0.20 Hz fre-

quency bin and occurred in the striatum (1) and the cortical (5 and 10) components. Additionally, cortical component 4 was significantly increased at the 0.12-0.16 Hz frequency. The significant decrease (PCP>Sal) occurred in striatal component 3 at 0.12-0.16 Hz.

4.2.8 Spectral Power - Statistical Analysis of Treatment Effects on Day 36

An investigation of the effects of treatment on spectral power was conducted on the data from the day 36 time point (see Figure 4.13B). These analyses investigate the effects of the treatment occur 10 days following the final injection. Again, the results were completed by subtracting the saline data from the PCP data (PCP-Sal). Trends throughout the day 36 results look similar to the results identified in the overall treatment t-tests (see Figure 4.13A). Overall, all of the components consistently displayed increases in spectral power for the PCP exposed rats (PCP>Sal) for the highest frequency bin of 0.20-0.24 Hz. As the frequency decreases the spectral power also decreases for most of the components. This results in the lowest frequency bins (0.00-0.04, 0.04-0.08, and 0.08-0.12) being comprised of increased spectral power in the saline rats (Sal>PCP). These analyses also revealed a total of 23 significant differences, 13 increases and 10 decreases ($p<0.05$ and $p<0.05/6$). Twelve out of the thirteen significant results were due to an increase in spectral power in the PCP exposed animals at 0.20-0.24 Hz. These significant differences occurred in the thalamic (1), cortical (1, 2, 4, 5, 6, 7, 8, and 10), hippocampal (3 and 4), and midbrain (1) components. The remaining increases in power occurred in hippocampal component 1 at 0.04-0.08 Hz. The ten significant increases in spectral power in the saline rats occurred primarily in the lower frequency bins. Five significant differences were identified at the 0.00-0.04 Hz frequency were in the thalamic (1), cortical (2, 5, and 6), and hippocampal (4) components. The hippocampal components 2 and 3 were sig-

nificant at 0.16-0.20 Hz and 0.04-0.08 Hz respectively. The three remaining increases in the saline rats occurred in the 0.08-0.12 frequency bins and were identified in the cerebellar component and cortical components 3 and 10.

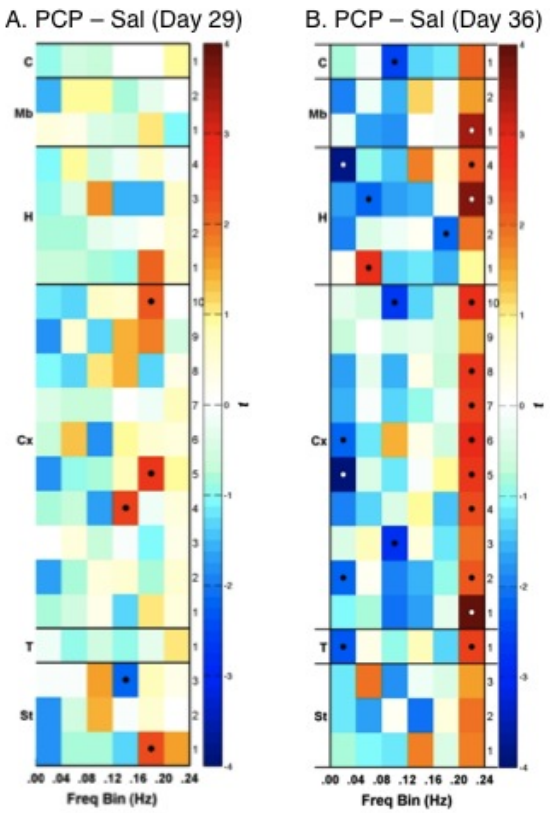

Figure 4.13: T-tests conducted to determine treatment effects on day 29 (A) and day 36 (B). Black dots indicate significance at $p<0.05$ and white dots indicate significance at $p<0.05/6$.

4.3 Morris Water Task

An alpha of $p<0.05$ was applied to all analyses and partial eta squared (η_p^2) are reported for all significant differences.

4.3.1 Pre-injection Training

Prior to the beginning of the injection regiment, all of the rats were pre-tested in the Morris Water Task (MWT). All animals received 16 hidden platform training trials. Separate repeated measures analysis of variance (ANOVAs) were conducted on the path lengths and latencies for all animals and trials (see Figure 4.14). Data were collapsed across scan time groups within treatment because there were no significant differences between the different scan time groups.

There was a significant effect of trial for path length (Greenhouse-Geisser corrected $F(6.932, 242.635) = 37.769$, $p<0.001$, $\eta_p^2 = 0.519$) and latency (Greenhouse-Geisser corrected $F(6.954, 264.241) = 41.048$, $p<0.001$, $\eta_p^2 = 0.519$). All animals achieved an asymptote in performance beginning around trial 8 and sufficiently learned the task in this training paradigm. There was not a significant trail by treatment interaction in path length (Greenhouse-Geisser corrected $F(6.932, 242.635) = 0.436$, $p=0.878$, $\eta_p^2 = 0.012$) or latency (Greenhouse-Geisser corrected $F(6.954, 264.241) = 0.500$, $p=0.833$, $\eta_p^2 = 0.013$) throughout the pre-injection training session. This result was expected and supports that any changes seen at the post-injection MWT testing session are due to the effect of the treatment.

4.3.2 Post-Injection Testing

Following the 4 weeks of injections, all of the animals were scanned in the MRI and half of the animals (N=20; sal=10, PCP=10) received testing in the MWT following this scan. The remaining half of the animals (N=20; sal=10, PCP=10) experienced a 1-week cessation period before receiving a second scan in the MRI followed by testing in the MWT. Because the animals were tested in the MWT after the final scan the data below are grouped into the animals that were tested following the initial scan on day 29 and the animals that were tested following the second scan on day 36.

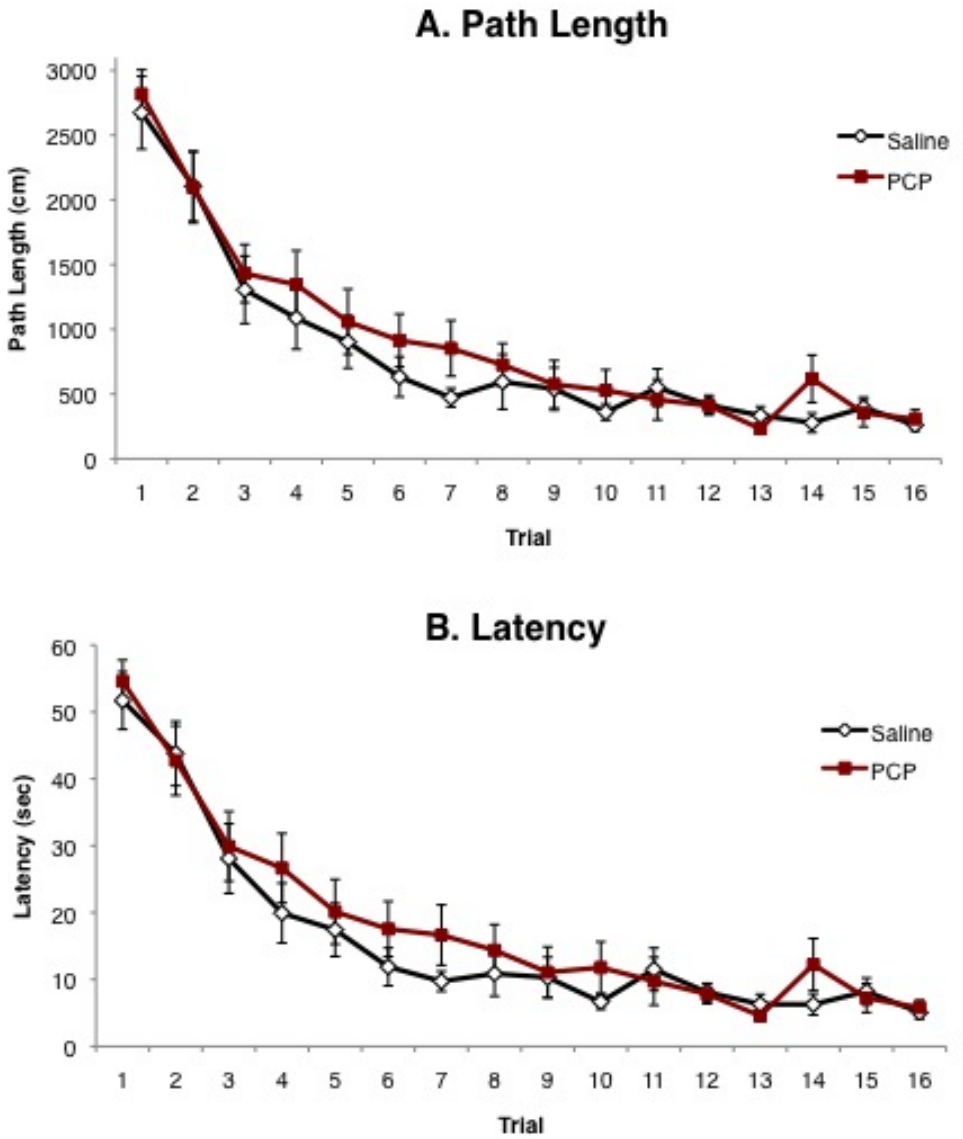

Figure 4.14: Pre-injection MWT training collapsed across scan time groups within each treatment group. Saline exposed animals are indicated by the open diamonds and PCP exposed animals are indicated by the closed red squares. The dependent measures are the length of the swim path (cm, A) and latency (sec, B) to reach the hidden platform location.

During the testing session, all of the animals were given 8 retraining trials, a break of at least 1 hour, 4 additional retraining trials, 8 reversal trials, and a no platform probe.

4.3.3 MWT Retraining Final Scan on Day 29

For the animals that received MWT testing after 1 scan (see Figure 4.15 A and B), there was a significant effect of trial for path length (Greenhouse-Geisser corrected $F(2.339, 42.099) = 10.959$, $p<0.001$, $\eta_p^2 = 0.378$) and latency (Greenhouse-Geisser corrected $F(1.993, 35.866) = 15.386$, $p<0.001$, $\eta_p^2 = 0.416$). All animals achieved an asymptote in performance beginning on trial 2 and sufficiently learned the task in the retraining session. There was not a significant trail by treatment interaction in path length (Greenhouse-Geisser corrected $F(2.339, 42.099) = 0.789$, $p=0.479$, $\eta_p^2 = 0.042$) or latency (Greenhouse-Geisser corrected $F(1.993, 35.866) = 0.713$, $p=0.497$, $\eta_p^2 = 0.038$) throughout the post-injection retraining session. On the first trial of the retraining session, the PCP exposed animals displayed a non-significant increased trend in path length and latency to reach the hidden platform. By trial 2, all of the animals began to behave in a similar manner and their latencies and path lengths began to asymptote. These data indicate that the animals were proficient in the task and were taking efficient swim paths to the hidden platform location.

4.3.4 MWT Retraining Final Scan on Day 36

For the animals that received MWT testing after a second scan (see Figure 4.15 C and D), there was a significant effect of trial for path length (Greenhouse-Geisser corrected $F(2.077, 37.388) = 7.317$, $p=0.002$, $\eta_p^2 = 0.289$) and latency (Greenhouse-Geisser corrected $F(1.868, 33.624) = 9.038$, $p=0.001$, $\eta_p^2 = 0.334$). Similar to the data from the first set (Day 29) of animals, all of the animals from the second cohort

achieved an asymptote in performance beginning on trial 2. There was not a significant trial by treatment interaction in path length (Greenhouse-Geisser corrected $F(2.077, 37.388) = 0.337$, $p=0.724$, $\eta_p^2 = 0.018$) or latency (Greenhouse-Geisser corrected $F(1.868, 33.624) = 0.272$, $p=0.748$, $\eta_p^2 = 0.015$) throughout the post-injection retraining session. Again, on the first trial of the retraining session, the PCP exposed animals displayed a non-significant increased trend in path length and latency to reach the hidden platform. The data from the second cohort of animals on trial 1 were non-significantly increased compared to the trial 1 data from the first cohort of animals. By trial 2, all of the two scan animals began to behave in a similar to that of the animals that received one scan and their latencies and path lengths began to asymptote. These data indicate that, despite the initial increase in latencies and path length on trial 1, all of the animals became proficient in the task and were taking efficient swim paths to the hidden platform location.

4.3.5 MWT Reversal Final Scan on Day 29

The reversal data from the animals that received MWT testing after 1 scan (see Figure 4.16 A and B) revealed a significant effect of trial for path length (Greenhouse-Geisser corrected $F(1.931, 34.754) = 16.823$, $p<0.001$, $\eta_p^2 = 0.483$) and latency (Greenhouse-Geisser corrected $F(1.671, 30.081) = 17.058$, $p<0.001$, $\eta_p^2 = 0.487$). Similar to the retraining data, all of the animals began to achieve asymptote in performance beginning on trial 2. There was not a significant trial by treatment interaction in path length (Greenhouse-Geisser corrected $F(1.931, 34.754) = 0.325$, $p=0.717$, $\eta_p^2 = 0.018$) or latency (Greenhouse-Geisser corrected $F(1.671, 30.081) = 0.310$, $p=0.697$, $\eta_p^2 = 0.017$) throughout the post-injection reversal session. Both the saline and PCP exposed animals displayed an increase in path length and latency in the initial reversal trial compared to the final retraining trial, which is expected. By trial 2, all of the animals began to perform in a similar manner and their latencies

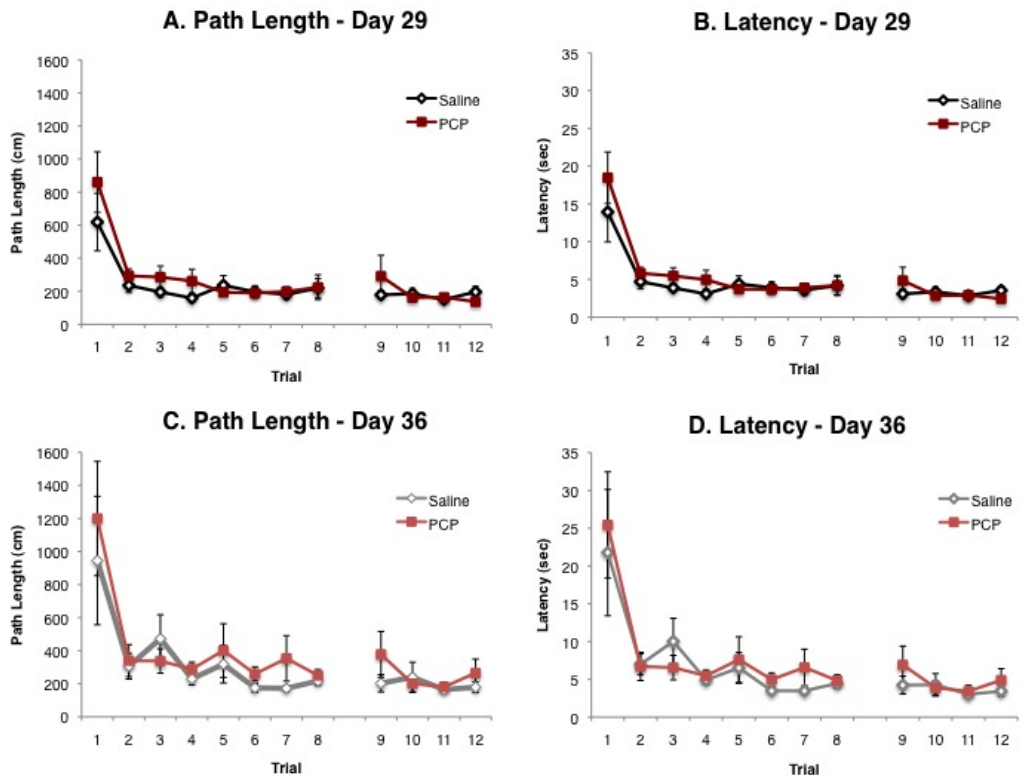

Figure 4.15: Post-injection MWT retraining for both treatment groups (A, B) without and (C, D) with the 1-week cessation period. Saline exposed animals are indicated by the open black and gray diamonds and PCP exposed animals are indicated by the closed red and pink squares. The dependent measures are the length of the swim path (cm, A and C) and latency (sec, B and D) to reach the hidden platform location.

and path lengths began to reach asymptotic levels. These data indicate that all of the animals, regardless of treatment group, were proficient in the reversal task and were taking efficient swim paths to the hidden platform location.

4.3.6 MWT Reversal - Final Scan on Day 36

The data from the animals that received MWT testing after a second scan (see Figure 4.16 C and D) also revealed a significant effect of trial for path length (Greenhouse-Geisser corrected $F(1.951, 35.118) = 17.076$, $p<0.001$, $\eta_p^2 = 0.487$) and latency (Greenhouse-Geisser corrected $F(1.818, 32.723) = 18.845$, $p<0.001$, $\eta_p^2 = 0.511$). There was not a significant trial by treatment interaction in path length (Greenhouse-Geisser corrected $F(1.951, 35.118) = 1.196$, $p=0.314$, $\eta_p^2 = 0.062$) or latency (Greenhouse-Geisser corrected $F(1.818, 32.723) = 1.502$, $p=0.238$, $\eta_p^2 = 0.077$) throughout the post-injection reversal session. There was an increase in path length and latency in the saline exposed animals similar to that found in the first cohort of animals. The PCP exposed animals displayed a non-significant reduced increase in path length and latency compared to all other groups. By trial 3, all of the two scan animals began to display an asymptote in a similar manner to that of the animals that received one scan. Additional measures such as initial heading trajectory, visits to the old training location, and time spent in the training and reversal regions were accessed for the reversal trials and the following no-platform probe trial and no differences were found between treatment and scan groups (data not shown).

4.4 Quantitative Real-Time PCR Results

The expressions of 6 genes highly implicated in schizophrenia were analyzed in brain tissue micro-dissected from the parietal cortex, medial frontal cortex, and ventral frontal cortex (see 4.17. Expressions of calbindin, GAD67, parvalbumin, ErbB4, GluN2A, and GluN2B mRNAs were normalized against levels of β-actin, which was used as a reference because its expression did not significantly vary between treatments or scan time groups.

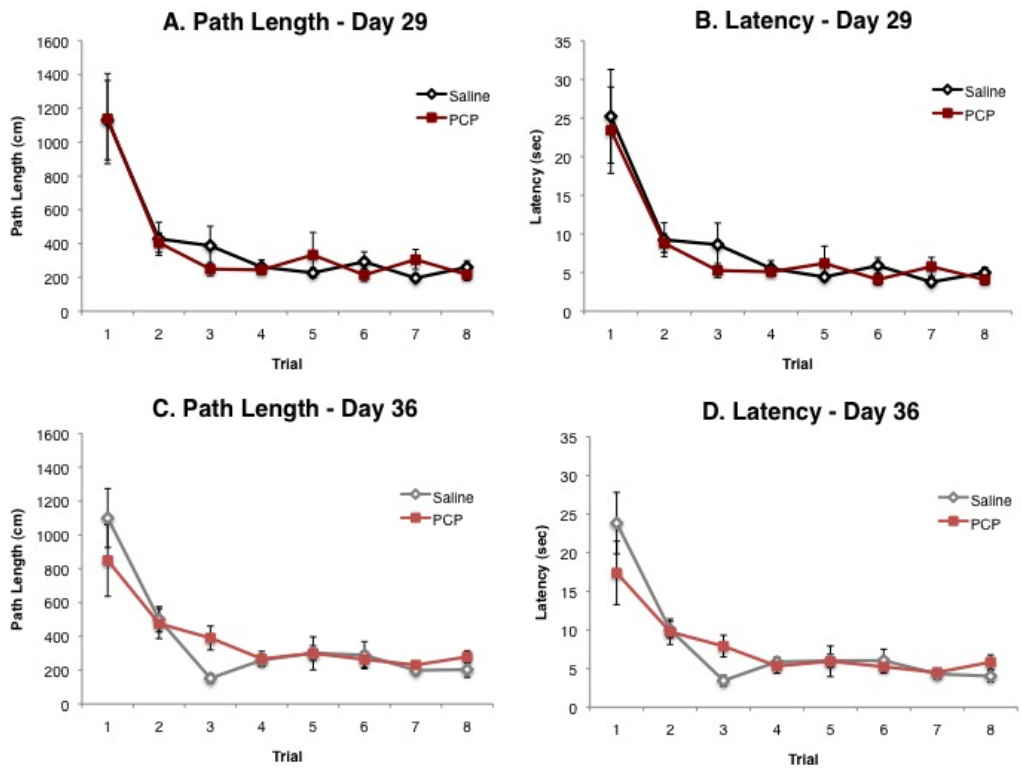

Figure 4.16: Post-injection MWT reversal for both treatment groups (A, B) without and (C, D) with the 1-week cessation period. Saline exposed animals are indicated by the open black and gray diamonds and PCP exposed animals are indicated by the closed red and pink squares. The dependent measures are the length of the swim path (cm, A and C) and latency (sec, B and D) to reach the hidden platform location.

A significant treatment by time interaction was observed in levels of parvalbumin expression in the parietal cortex ($F = 6.157$, $df = 1,37$, $p=0.018$) (see Figure 4.18 A). For the animals that received only 1 scan, the PCP exposed animals displayed an increased expression of parvalbumin compared to the control animals. Inversely, the PCP exposed animals that received 2 scans showed decreased expression of parvalbumin compared to the control animals that experienced the same timeline. Within treatment conditions, the expression of parvalbumin was significantly different be-

		Treatment Effect			Scan Effect			Treatment*Scan Interaction		
Front Ventral		F Value	df	P Value	F Value	df	P Value	F Value	df	P Value
	Calbindin	0.165	1, 39	0.687	2.831	1, 39	0.101	**3.09**	**1, 39**	**0.087**
	GAD67	1.266	1, 39	0.268	0.324	1, 39	0.573	1.134	1, 39	0.294
	Parvalbumin	0.079	1, 39	0.78	0.604	1, 39	0.442	0.049	1, 39	0.826
	ErbB4	2.61	1, 39	0.115	0	1, 39	0.993	0.484	1, 39	0.491
	GluN2A	2.33	1, 39	0.136	0.002	1, 39	0.964	2.014	1, 39	0.164
	GluN2B	2.43	1, 39	0.128	0.124	1, 39	0.727	0.12	1, 39	0.731
Front Medial		F Value	df	P Value	F Value	df	P Value	F Value	df	P Value
	Calbindin	**3.461**	**1, 39**	**0.071**	0.188	1, 39	0.667	1.287	1, 39	0.264
	GAD67	0.03	1, 39	0.864	0.116	1, 39	0.736	0.567	1, 39	0.456
	Parvalbumin	0.6	1, 39	0.444	0.273	1, 39	0.604	0.608	1, 39	0.441
	ErbB4	0.035	1, 39	0.852	1.433	1, 39	0.239	1.981	1, 39	0.168
	GluN2A	0.089	1, 39	0.767	0.032	1, 39	0.859	0.205	1, 39	0.653
	GluN2B	0.18	1, 39	0.674	0.164	1, 39	0.687	0.557	1, 39	0.46
Parietal Cortex		F Value	df	P Value	F Value	df	P Value	F Value	df	P Value
	Calbindin	0.1	1, 39	0.754	0.048	1, 39	0.828	0.48	1, 39	0.493
	GAD67	**3.586**	**1, 39**	**0.066**	0.41	1, 39	0.526	0.114	1, 39	0.738
	Parvalbumin	0.631	1, 37	0.433	0.007	1, 37	0.932	**6.157**	**1, 37**	**0.018**
	ErbB4	0.017	1, 39	0.898	2.262	1, 39	0.141	0.999	1, 39	0.324
	GluN2A	0.753	1, 39	0.391	1.461	1, 39	0.235	1.421	1, 39	0.241
	GluN2B	0.092	1, 39	0.763	0.01	1, 39	0.921	0.744	1, 39	0.394

Figure 4.17: Summary of analyses investigating treatment main effects, time main effects, and treatment by scan time interactions in mRNA expression levels of calbindin, GAD67, parvalbumin, ErbB4, GluN2A, and GluN2B in the medial frontal cortex, ventral frontal cortex, and parietal cortex.

tween animals that received one scan and those that were allowed a cessation period between the two scans. PCP exposed animals displayed a decreased expression between the two scanning groups while the control animals displayed an increased expression between groups.

In both scan groups the PCP exposed animals had decreased expression of GAD_{67} mRNA in the parietal cortex (see Figure 4.18 B) compared to saline exposed control animals although it was not significant (F = 3.586, df = 1,39, p=0.066).

Additionally, we observed a trend for increased levels of calbindin in the medial frontal cortex (see Figure 4.18 C) in the PCP exposed animals for both scan groups when compared to the control animals, but the difference was not significant (F = 3.461, df = 1,39, p=0.071).

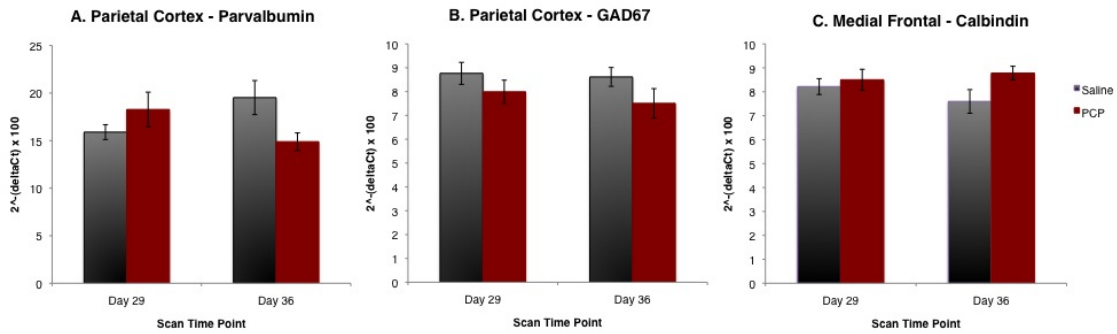

Figure 4.18: Relative mRNA expression levels of (A) parvalbumin and (B) GAD_{67} in the parietal cortex and (C) calbindin in the medial frontal cortex.

Chapter 5

Discussion

Repeated exposure to a low dose of PCP resulted in connectivity, spectral power, mild behavioral, and mRNA expression changes in the rodent system. First, we were able to successfully identify 21 independent non-artifactual components from the EPI data and assess resting-state functional network connectivity in rodent systems exposed to saline and PCP. The present study discovered that sub-chronic sub-intermittent exposure to PCP results in persistent FNC changes in a rat model. The treatment effects present on day 29 suggests that PCP alters connectivity with in cortical regions and between the cortex, striatum, and midbrain. Specifically, the significant relationships between the cortex and striatum and within cortical regions are increased in the PCP exposed animals and the relationship between the cortex and the midbrain was decreased in the PCP exposed animals. There are also trends for increased correlational strength in the PCP group on day 29 throughout the relationships between the striatum and the hippocampus, midbrain, and cerebellum. These increases are also found within cortical components, between cortical-hippocampus components, and between cortical-midbrain components.

In regards to the data that addresses the wash-out period, the PCP exposed

animals showed an increased number of significant relationships on day 36 compared to the saline exposed animals. These findings suggest that PCP exposure results in increased hyperconnectivity that is persistent after the wash-out period. In the PCP exposed rats, there were similar connectivity trends for both day 29 and 36. There were strong positive correlations in the striatal-cortical, hippocampus-midbrain, midbrain-cerebellum, striatal-striatal, and cortical-cortical component relationships. Additionally, there were strong negative correlations in the striatal-hippocampal, striatal-midbrain, cortical-hippocampal, cortical-midbrain, and anterior cortical-cerebellar component relationships. These negative correlations were also present in the relationships between the striatum-thalamic components and between the anterior hippocampus and the midbrain and the cerebellum. When comparing the washout period in the saline group and the PCP group there were several noticeable differences between the two treatment groups. For example, the saline exposed displayed trends of negative correlations within the cortical components while the PCP exposed animals displayed an increased number of positive correlations within the cortical components. Also, when examining the significant relationships only, the PCP group displayed the inverse of what the saline group displayed. The significant relationships from the wash-out period were primarily negative in the saline groups and primarily positive in the PCP exposed group. The increased correlational strength found in the PCP exposed animals may be indicative of the hyperconnectivity found in the schizophrenia population [20,38,39]. These changes are likely attributable to the functional consequences of the treatment because there were no structural differences in overall brain volume. This work is novel in that it addresses FNC and spectral power changes in a rodent sub-chronically and sub-intermittently exposed to a low dose of PCP as opposed to the current host of literature that addresses MRI in exposures to acute and higher doses of PCP [5,9,27].

The persistent effects of the PCP exposure were also present in the spectral power data. The initial scans on day 29 showed an increased power in the mid to

high frequency bins (0.12-0.16 and 0.16-0.20 Hz) in the PCP exposed rats. Most of the significant findings were indicative of the PCP group having a stronger power compared to the saline group and occurred in the cortex and the anterior striatum components. There were also trends for decreased power in the lower frequency bins for the PCP exposed rats. These findings were exacerbated after the wash-out period. The highest frequency bin (0.20-0.24 Hz) was consistently increased throughout all of the components in the PCP exposed animals. Most of the lower frequencies, especially the 0.00-0.04 Hz, had a decreased power for the PCP group. These outcomes suggest that there is an increased number of persistent changes in the PCP exposed animals compared to the saline exposed animals.

All of the rats had similar path lengths and latencies in the pre-injection MWT training session. The initial training session was successful in establishing a consistent baseline amongst all animals. Because all of the animals performed well in the initial training session, any changes found in the post-scan testing can be attributed to the treatment. The animals that received a washout period had increased path lengths and latencies in trial 1 of the post scan testing compared to the animals that were tested after the scan on day 29. This change could be due to the additional week that the animals had to forget the trained platform location. Despite the initial increased time and path length to find the hidden platform all of the animals from both time periods reached criterion throughout during the MWT post-scan testing. The rats that had the additional scan had slightly increased latencies and path lengths during the first 8 trials of the retraining session, but these differences were minimal and non-significant. All animals performed in an almost identical manner during the retraining session following the hour break. Furthermore, there were no significant differences in performance between the treatment groups and scan time groups during the reversal testing session. The null results throughout the MWT testing phase indicate that there were not detectable differences between the saline and PCP exposed animals in spatial memory or flexible behavior. The lack of

behavioral differences in memory could be due to the long time period (4 weeks) in between the training and testing sessions. The expected effects of PCP on flexible behavior were not obtained, which may be due to the treatment parameters along with the possibility that behavioral flexibility in the spatial domain might reflect compensation by neural systems not affected by PCP.

Some of the changes in mRNA expression are consistent with previously published results. The decreased expression of parvalbumin and GAD_{67} in the PCP groups are consistent with the findings of several animal model and post-mortem clinical studies [10,11,25]. The initial increase in parvalbumin mRNA in animals that received 1 scan and the increases in calbindin mRNA in the PCP exposed rats are counterintuitive to studies that have found decreases in parvalbumin [4, 47, 48] and calbindin [25]. The inconsistent changes could be due to the fact that the present study was conducted in adulthood when the expression of these genes are stable and fairly resilient to the low dose of PCP that was administered.

There are a host of directions and modifications that this study could address in the future in order to identify additional PCP induced changes. First, additional analyses could be conducted on the fMRI data. A seed based or graph theory approach could be applied in order to focus in on more specific regions of interest. Analyses of structural changes in overall gray matter or white matter tracts could be undertaken to determine if there are structural changes associated with the functional changes found in this study. Second, there could be additional behavioral tasks incorporated throughout the paradigm. For example, the animals could be tested in the MWT on a weekly basis in order to avoid the long gap between MWT sessions. Further, more sensitive behavioral tasks and/or measures could be utilized. Third, additional qRT-PCR analyses could be conducted in other brain regions, such as the hippocampus. Expression of other genes associated with schizophrenia could be measured in the regions that were used in this study and/or in additional tissue.

Finally, this paradigm could be used in younger animals to determine if these changes are exacerbated in a developing system. Overall, this study suggests that exposure to PCP results in connectivity, behavioral, and gene expression changes that are similar to those found in other animal models and the clinical schizophrenia population. These methods may be used to help differentiate between PCP and saline exposed animals and could help identify some underlying mechanisms in schizophrenia.

In summary, we were able to differentiate the PCP treated rats from the control animals through examination of fMRI and mRNA analyses. We successfully identified persistent connectivity changes in the PCP exposed rats compared to the saline exposed rats. Persistent changes were also present in spectral power data. Although we did not see any behavioral changes in the MWT, the PCP exposed animals displayed altered mRNA expression levels of parvalbumin, GAD_{67}, and calbindin. These changes are similar to some aspects of the human schizophrenia and other animal models that utilize manipulations of NMDARs, but additional research is needed in order to make this model more indicative of the clinical schizophrenia population.

References

[1] Z Abdul-Monim, J C Neill, and G P Reynolds. Sub-chronic psychotomimetic phencyclidine induces deficits in reversal learning and alterations in parvalbumin-immunoreactive expression in the rat. *J Psychopharmacol*, 21(2):198–205, Mar 2007.

[2] Z Abdul-Monim, G P Reynolds, and J C Neill. The effect of atypical and classical antipsychotics on sub-chronic pcp-induced cognitive deficits in a reversal-learning paradigm. *Behav Brain Res*, 169(2):263–73, May 2006.

[3] Elena A Allen, Erik B Erhardt, Eswar Damaraju, William Gruner, Judith M Segall, Rogers F Silva, Martin Havlicek, Srinivas Rachakonda, Jill Fries, Ravi Kalyanam, Andrew M Michael, Arvind Caprihan, Jessica A Turner, Tom Eichele, Steven Adelsheim, Angela D Bryan, Juan Bustillo, Vincent P Clark, Sarah W Feldstein Ewing, Francesca Filbey, Corey C Ford, Kent Hutchison, Rex E Jung, Kent A Kiehl, Piyadasa Kodituwakku, Yuko M Komesu, Andrew R Mayer, Godfrey D Pearlson, John P Phillips, Joseph R Sadek, Michael Stevens, Ursina Teuscher, Robert J Thoma, and Vince D Calhoun. A baseline for the multivariate comparison of resting-state networks. *Front Syst Neurosci*, 5:2, 2011.

[4] Nurith Amitai, Ronald Kuczenski, M Margarita Behrens, and Athina Markou. Repeated phencyclidine administration alters glutamate release and decreases gaba markers in the prefrontal cortex of rats. *Neuropharmacology*, 62(3):1422–31, Mar 2012.

[5] Samuel A Barnes, Stephen J Sawiak, Daniele Caprioli, Bianca Jupp, Guido Buonincontri, Adam C Mar, Michael K Harte, Paul C Fletcher, Trevor W Robbins, Jo C Neill, and Jeffrey W Dalley. Impaired limbic cortico-striatal structure and sustained visual attention in a rodent model of schizophrenia. *Int J Neuropsychopharmacol*, 18(2), Jan 2015.

[6] Simret Beraki, Alexander Kuzmin, Fadao Tai, and Sven Ove Ogren. Repeated low dose of phencyclidine administration impairs spatial learning in mice: blockade by clozapine but not by haloperidol. *Eur Neuropsychopharmacol*, 18(7):486–97, Jul 2008.

[7] Monica M Bolton, Chelcie F Heaney, Jonathan J Sabbagh, Andrew S Murtishaw, Christy M Magcalas, and Jefferson W Kinney. Deficits in emotional learning and memory in an animal model of schizophrenia. *Behav Brain Res*, 233(1):35–44, Jul 2012.

[8] B L Brim, R Haskell, R Awedikian, N M Ellinwood, L Jin, A Kumar, T C Foster, and K R Magnusson. Memory in aged mice is rescued by enhanced expression of the glun2b subunit of the nmda receptor. *Behav Brain Res*, 238:211–26, Feb 2013.

[9] Brian V Broberg, Kristoffer H Madsen, Niels Plath, Christina K Olsen, Birte Y Glenthøj, Olaf B Paulson, Börje Bjelke, and Lise V Søgaard. A schizophrenia rat model induced by early postnatal phencyclidine treatment and characterized by magnetic resonance imaging. *Behav Brain Res*, 250:1–8, Aug 2013.

[10] W Michael Bullock, Federico Bolognani, Paolo Botta, C Fernando Valenzuela, and Nora I Perrone-Bizzozero. Schizophrenia-like gabaergic gene expression deficits in cerebellar golgi cells from rats chronically exposed to low-dose phencyclidine. *Neurochem Int*, 55(8):775–82, Dec 2009.

[11] W Michael Bullock, Karen Cardon, Juan Bustillo, Rosalinda C Roberts, and Nora I Perrone-Bizzozero. Altered expression of genes involved in gabaergic transmission and neuromodulation of granule cell activity in the cerebellum of schizophrenia patients. *Am J Psychiatry*, 165(12):1594–603, Dec 2008.

[12] Jeffrey Burgdorf, Xiao-lei Zhang, Craig Weiss, Elizabeth Matthews, John F Disterhoft, Patric K Stanton, and Joseph R Moskal. The n-methyl-d-aspartate receptor modulator glyx-13 enhances learning and memory, in young adult and learning impaired aging rats. *Neurobiol Aging*, 32(4):698–706, Apr 2011.

[13] J R Bustillo, J Lauriello, and S J Keith. Schizophrenia: improving outcome. *Harv Rev Psychiatry*, 6(5):229–40, 1999.

[14] Juan Bustillo, Matthew P Galloway, Farhad Ghoddoussi, Federico Bolognani, and Nora Perrone-Bizzozero. Medial-frontal cortex hypometabolism in chronic phencyclidine exposed rats assessed by high resolution magic angle spin 11.7 t proton magnetic resonance spectroscopy. *Neurochem Int*, 61(1):128–31, Jul 2012.

[15] Philip E Chen, Michael L Errington, Matthias Kneussel, Guiquan Chen, Alexander J Annala, York H Rudhard, Georg F Rast, Christian G Specht, Cezar M Tigaret, Mohammed A Nassar, Richard G M Morris, Timothy V P Bliss, and Ralf Schoepfer. Behavioral deficits and subregion-specific suppression of LTP in mice expressing a population of mutant nmda receptors throughout the hippocampus. *Learn Mem*, 16(10):635–44, Oct 2009.

[16] Susan M Cochran, Matthew Kennedy, Clare E McKerchar, Lucinda J Steward, Judith A Pratt, and Brian J Morris. Induction of metabolic hypofunction and neurochemical deficits after chronic intermittent exposure to phencyclidine: differential modulation by antipsychotic drugs. *Neuropsychopharmacology*, 28(2):265–75, Feb 2003.

[17] N M W J de Bruin, M van Drimmelen, M Kops, J van Elk, M Middelveld-van de Wetering, and I Schwienbacher. Effects of risperidone, clozapine and the 5-ht6 antagonist gsk-742457 on pcp-induced deficits in reversal learning in the two-lever operant task in male sprague dawley rats. *Behav Brain Res*, 244:15–28, May 2013.

[18] Teresa Marie du Bois, Kelly Anne Newell, and Xu-Feng Huang. Perinatal phencyclidine treatment alters neuregulin 1/erbb4 expression and activation in later life. *Eur Neuropsychopharmacol*, 22(5):356–63, May 2012.

[19] Alice Egerton, Lee Reid, Sandie McGregor, Susan M Cochran, Brian J Morris, and Judith A Pratt. Subchronic and chronic pcp treatment produces temporally distinct deficits in attentional set shifting and prepulse inhibition in rats. *Psychopharmacology (Berl)*, 198(1):37–49, May 2008.

[20] Paul J Fitzgerald. The nmda receptor may participate in widespread suppression of circuit level neural activity, in addition to a similarly prominent role in circuit level activation. *Behav Brain Res*, 230(1):291–8, Apr 2012.

[21] Abigail G Garrity, Godfrey D Pearlson, Kristen McKiernan, Dan Lloyd, Kent A Kiehl, and Vince D Calhoun. Aberrant "default mode" functional connectivity in schizophrenia. *Am J Psychiatry*, 164(3):450–7, Mar 2007.

[22] Francois Gastambide, Stephen N Mitchell, Trevor W Robbins, Mark D Tricklebank, and Gary Gilmour. Temporally distinct cognitive effects following acute administration of ketamine and phencyclidine in the rat. *Eur Neuropsychopharmacol*, Apr 2013.

[23] M A Geyer, K Krebs-Thomson, D L Braff, and N R Swerdlow. Pharmacological studies of prepulse inhibition models of sensorimotor gating deficits in

schizophrenia: a decade in review. *Psychopharmacology (Berl)*, 156(2-3):117–54, Jul 2001.

[24] Alexandre Duarte Gigante, David J Bond, Beny Lafer, Raymond W Lam, L Trevor Young, and Lakshmi N Yatham. Brain glutamate levels measured by magnetic resonance spectroscopy in patients with bipolar disorder: a meta-analysis. *Bipolar Disord*, 14(5):478–87, Aug 2012.

[25] Javier Gilabert-Juan, Maria Belles, Ana Rosa Saez, Hector Carceller, Sara Zamarbide-Fores, Maria Dolores Moltó, and Juan Nacher. A "double hit" murine model for schizophrenia shows alterations in the structure and neurochemistry of the medial prefrontal cortex and the hippocampus. *Neurobiol Dis*, 59:126–40, Nov 2013.

[26] Gary Gilmour, Sophie Dix, Laetitia Fellini, Francois Gastambide, Niels Plath, Thomas Steckler, John Talpos, and Mark Tricklebank. Nmda receptors, cognition and schizophrenia–testing the validity of the nmda receptor hypofunction hypothesis. *Neuropharmacology*, 62(3):1401–12, Mar 2012.

[27] Alessandro Gozzi, Hugh Herdon, Adam Schwarz, Simone Bertani, Valerio Crestan, Giuliano Turrini, and Angelo Bifone. Pharmacological stimulation of nmda receptors via co-agonist site suppresses fmri response to phencyclidine in the rat. *Psychopharmacology (Berl)*, 201(2):273–84, Dec 2008.

[28] Faith M Hanlon, Michael P Weisend, Derek A Hamilton, Aaron P Jones, Robert J Thoma, Mingxiong Huang, Kimberly Martin, Ronald A Yeo, Gregory A Miller, and Jose M Cañive. Impairment on the hippocampal-dependent virtual morris water task in schizophrenia. *Schizophr Res*, 87(1-3):67–80, Oct 2006.

[29] R Matthew Hutchison, Seyed M Mirsattari, Craig K Jones, Joseph S Gati, and L Stan Leung. Functional networks in the anesthetized rat brain revealed by independent component analysis of resting-state fmri. *J Neurophysiol*, 103(6):3398–406, Jun 2010.

[30] D C Javitt and S R Zukin. Recent advances in the phencyclidine model of schizophrenia. *Am J Psychiatry*, 148(10):1301–8, Oct 1991.

[31] Daniel C Javitt, Stephen R Zukin, Uriel Heresco-Levy, and Daniel Umbricht. Has an angel shown the way? etiological and therapeutic implications of the pcp/nmda model of schizophrenia. *Schizophr Bull*, 38(5):958–66, Sep 2012.

[32] C A Jones, D J G Watson, and K C F Fone. Animal models of schizophrenia. *Br J Pharmacol*, 164(4):1162–94, Oct 2011.

[33] Ye-Ha Jung and Yoo-Hun Suh. Differential functions of nr2a and nr2b in short-term and long-term memory in rats. *Neuroreport*, 21(12):808–11, Aug 2010.

[34] Dae Il Kim, D H Mathalon, J M Ford, M Mannell, J A Turner, G G Brown, A Belger, R Gollub, J Lauriello, C Wible, D O'Leary, K Lim, A Toga, S G Potkin, F Birn, and V D Calhoun. Auditory oddball deficits in schizophrenia: an independent component analysis of the fmri multisite function birn study. *Schizophr Bull*, 35(1):67–81, Jan 2009.

[35] A C Lahti, M A Weiler, B A Tamara Michaelidis, A Parwani, and C A Tamminga. Effects of ketamine in normal and schizophrenic volunteers. *Neuropsychopharmacology*, 25(4):455–67, Oct 2001.

[36] D S Manoach, R L Gollub, E S Benson, M M Searl, D C Goff, E Halpern, C B Saper, and S L Rauch. Schizophrenic subjects show aberrant fmri activation of dorsolateral prefrontal cortex and basal ganglia during working memory performance. *Biol Psychiatry*, 48(2):99–109, Jul 2000.

[37] Bita Moghaddam and Daniel Javitt. From revolution to evolution: the glutamate hypothesis of schizophrenia and its implication for treatment. *Neuropsychopharmacology*, 37(1):4–15, Jan 2012.

[38] Rodrigo D Paz, Nancy C Andreasen, Sami Z Daoud, Robert Conley, Rosalinda Roberts, Juan Bustillo, and Nora I Perrone-Bizzozero. Increased expression of activity-dependent genes in cerebellar glutamatergic neurons of patients with schizophrenia. *Am J Psychiatry*, 163(10):1829–31, Oct 2006.

[39] S G Potkin, J A Turner, G G Brown, G McCarthy, D N Greve, G H Glover, D S Manoach, A Belger, M Diaz, C G Wible, J M Ford, D H Mathalon, R Gollub, J Lauriello, D O'Leary, T G M van Erp, A W Toga, A Preda, K O Lim, and FBIRN. Working memory and dlpfc inefficiency in schizophrenia: the fbirn study. *Schizophr Bull*, 35(1):19–31, Jan 2009.

[40] Jonathan J Sabbagh, Chelcie F Heaney, Monica M Bolton, Andrew S Murtishaw, and Jefferson W Kinney. Examination of ketamine-induced deficits in sensorimotor gating and spatial learning. *Physiol Behav*, 107(3):355–63, Oct 2012.

[41] Thomas D Schmittgen and Kenneth J Livak. Analyzing real-time pcr data by the comparative c(t) method. *Nat Protoc*, 3(6):1101–8, 2008.

[42] Petra Schweinhardt, Peter Fransson, Lars Olson, Christian Spenger, and Jesper L R Andersson. A template for spatial normalisation of mr images of the rat brain. *J Neurosci Methods*, 129(2):105–13, Oct 2003.

[43] Annalisa Scimemi, James S Meabon, Randall L Woltjer, Jane M Sullivan, Jeffrey S Diamond, and David G Cook. Amyloid-1-42 slows clearance of synaptically released glutamate by mislocalizing astrocytic glt-1. *J Neurosci*, 33(12):5312–5318, Mar 2013.

[44] Janice W Smith, Francois Gastambide, Gary Gilmour, Sophie Dix, Julie Foss, Kirstie Lloyd, Nadia Malik, and Mark Tricklebank. A comparison of the effects of ketamine and phencyclidine with other antagonists of the nmda receptor in rodent assays of attention and working memory. *Psychopharmacology (Berl)*, 217(2):255–69, Sep 2011.

[45] Jason Smucny, Korey P Wylie, and Jason R Tregellas. Functional magnetic resonance imaging of intrinsic brain networks for translational drug discovery. *Trends Pharmacol Sci*, 35(8):397–403, Aug 2014.

[46] Eva M. Tsapakis and Michael J. Travis. Glutamate and psychiatric disorders. *Advances in Psychiatric Treatment*, 8:189–197, 2002.

[47] Dong Xi, Wentong Zhang, Huai-Xing Wang, George G Stradtman, and Wen-Jun Gao. Dizocilpine (mk-801) induces distinct changes of n-methyl-d-aspartic acid receptor subunits in parvalbumin-containing interneurons in young adult rat prefrontal cortex. *Int J Neuropsychopharmacol*, 12(10):1395–408, Nov 2009.

[48] Jian-Ming Yang, Jing Zhang, Xiao-Juan Chen, Hong-Yan Geng, Mao Ye, Nicholas C Spitzer, Jian-Hong Luo, Shu-Min Duan, and Xiao-Ming Li. Development of gaba circuitry of fast-spiking basket interneurons in the medial prefrontal cortex of erbb4-mutant mice. *J Neurosci*, 33(50):19724–33, Dec 2013.